# AN EXPERIMENTAL INVESTIGATION OF THE GAINS OF DIELECTRIC ANTENNAS

R. B. JOHNSTON

AN EXPERIMENTAL INVESTIGATION OF THE GAINS OF

DIELECTRIC ANTENNAS

by

Robert Bruce Johnston

An essay submitted to the Advisory Board of the School of Engineering, The Johns Hopkins University, in conformity with the requirement for the degree of Master of Science in Engineering

Baltimore, Maryland

1952

## ACKNOWLEDGEMENTS

The author wishes to express his grateful appreciation to Dr. Gilbert Wilkes of The Johns Hopkins University Applied Physics Laboratory, where this experimental work was performed, for stimulation of interest in this problem and for his continued interest and capable guidance throughout the work. This work was supported by the Bureau of Ordnance, U.S. Navy, under Contract NOrd 7386.

Thanks are also due to Professor Randolph Church of the U.S. Naval Postgraduate School for counsel on the construction of the nomogram for solution of the equation for waves in a circular cylinder.

18040

# TABLE OF CONTENTS

# AN EXPERIMENTAL INVESTIGATION OF THE GAINS OF DIELECTRIC ANTENNAS

## INTRODUCTION

The idea of using dielectric materials for the control of the direction of electromagnetic radiation was probably first conceived by Hertz in the Nineteenth Century[1], when he observed the strong influence of pitch blocks on this little understood form of energy flow. Subsequently, in the early part of the Twentieth Century a few investigations were reported concerning the use of dielectrics as wave guides, but there were only occasional contributions to this theory. Rapid progress in this direction was not begun until the availability of microwave equipment in the 1930's. By 1939, dielectric wave guide theory had been thoroughly studied and a few experiments had been attempted in the use of dielectrics as directional radiators. With the stimulus of the war, and the rapidly increasing need for more highly directive antennas, dielectric rods were studied,

1. Superscript numbers refer to references listen in Bibliography.

tried, and put into use beginning in the early 1940's. In 1943 the U.S. Navy put into service a radar equipment, designed by the Bell Telephone Laboratories, which employed an array of forty-two rods of Polystyrene to give a sharp directional beam in the horizontal plane. (Radar Equipment Mark VIII). The Germans, about the same time, began to use a directional antenna on aircraft[2] which consisted of four dielectric rods arranged to give a symmetrical pattern. Subsequently, a large number of dielectric antennas have been built, and an ever increasing demand for these small size, highly directional devices has encouraged more and more attention to their theory of operation.

It should be pointed out in the beginning that the classical methods of antenna design, based on Maxwell's equations, have not been successfully applied to dielectric antennas whose dimensions have been of the order of a wavelength. As clearly pointed out by Stratton[3] in his book, "Electromagnetic Theory", Maxwell's equations are valid, in general, only to large scale phenomena, and attempts to extend them to the so called "Quasi-microscopic state" lead only to partial success. Although many of the laws of

classical electrodynamics apply to submicroscopic domains, it is not possible to apply them generally. On the other side, there is quantum electrodynamics, which at this writing, have not been extended through the transition areas. The statistical averages, over a large number of atoms, of the equations of quantum electrodynamics ultimately must lead to the relations derived by Maxwell.

Design of dielectric antennas to date has been based largely on cut and try methods. Some of their characteristics have been determined by various experimenters, and considerable theoretical work has been done in an endeavor to explain their operation. But there is no mass of data for the theorist to draw upon, nor is there an adequate theory at the present time to enable calculation or prediction of the characteristics of a given dielectric shape. It is the purpose of the writer, in undertaking this work, to determine experimentally the "concentrating action" of certain of these antennas, and to express this in terms of gain relative to an isotropic oscillator; or, what amounts to the same thing, to express this gain as a ratio of effective area to actual area. It is believed that these data, thus

obtained, may be of use in subsequent investigations, or for other investigators, to ultimately develop a satisfactory theory of the function of the dielectric antenna. Finally, available theoretical approaches will be discussed objectively in the light of the experimental results obtained herein.

Work of other investigators:

Mallach[6], in Germany, presented a thesis in 1939 which reported considerable work in the use of dielectrics to produce a directional beam. He also produced a simple theory which explains qualitatively the action of the dielectric, but failed quantitatively to verify all of the known data. Taking a dielectric filled wave guide, whose walls are considered perfectly conducting, excited at one end and open at the other, it is well known that radiation is emitted from the open end, and this radiation is directional along the projected axis of the guide. If the conducting sheath is removed from a part of the guide, nearest the open end, leaving some of the dielectric rod protruding, radiation will occur both from the end of the dielectric and from its side walls as well. Mallach's theory is based on the consideration

that each element of the surface acts as a radiator and the phase of this excitation depends on the extended length of the rod. He assumes in this work that the wave is linearly polarized and of constant intensity and is transmitted down the rod without attenuation or reflection. Furthermore, he does not consider the rod cross section area except for the determination of the wavelength. He also considers only small angles of diffraction, taking no account of the spherical nature of the wave. Mallach reported a considerable amount of experimental data on both rods and dielectric tubes, and arrived at some simple formulas for choosing dimensions. For the sizes of rods and tubes that he used, his simple theory and formulas are satisfactory, but are of no use in obtaining lobe patterns for the entire radiation field nor for computing gains.

Southworth[7], at the Bell Telephone Laboratories, whose early publications on wave guides and wave guide theory are well known, has done considerable experimenting for more than a decade with tapered dielectric rods, both rectangular and circular, of diameters of a half wavelength or less. He and his associates have experimentally established that

the gain decreases as the attenuation in the rod increases.

Wilkes[8], in a thesis presented to the University of Paris in 1946, examined the problem from the point of view of the lens action of the dielectric on radiation of wavelèngths comparable to the dimensions of the lens. He pointed out that the apparent index of refraction plays an important role in the energy gain of the dielectric radiator. By plotting experimentally obtained energy gains versus length of exposed dielectric he has shown a correspondence of periodic gain to Snell's law of refraction. Furthermore he has shown that the apparent index of refraction is itself not constant, but depends on the exposed length of dielectric and a cross section dimension. A formula for calculating the apparent index from the real index of refraction is developed in his paper. Wilkes also computed some radiation patterns based on analogy to more conventional antennas, which verified very nicely the experimental data for the major lobe. But, as his paper points out, his assumptions used would cause considerable errors in the side lobes. This

calculation assumes constant wavelength, which he shows to vary somewhat throughout the lens length. He also assumes, for this calculation, constant displacement currents. The complexity of an exact formulation of wavelength and intensity would lead to expressions which would be extremely difficult if not impossible to solve.

Several investigators[11,12,16] have subsequently published attempts at calculation of radiation patterns. All of the recent attempts known to the author are based on the formal solution of the field equations given in Schelkunoff's well known book[4], as applied to waves in dielectric wires, and expressed in terms of cylinder functions. Elsasser[9] in 1949 published an analysis of the various non-radiative modes in a circular dielectric rod, in which he also pointed out a perturbation method of calculating dielectric loss. Elsasser, in this paper, did not attempt calculation of radiation from a finite length rod. This theoretical study is in substantial agreement with an experimental investigation of dielectric cylinders as wave guides performed by Chandler[10] at RCA laboratories.

Marston[11] of the U.S. Naval Research Laboratory has attempted calculation of radiation from dielectric rods of uniform circular cross section. He employed the method of assumed fields based on Schelkunoff's Equivalence theorems[18], published in the Bell System Technical Journal in 1936. Marston computed the radiation field arising from equivalent sources at the sides of the rod, and separately for those at the ends of the rod, and points out that maximum gain in the axial direction is achieved when the total radiation from the end is in phase with the radiation from sides (for modes of type $n = 1$ only). Marston's calculations also show that the actual values of gain for dielectric circular rods cannot in general be predicted from ordinary array theory, but prospects of achieving this exist through the use of his complex expressions for the components of electric field intensity. However, all of Marston's assumptions are not in agreement with findings of other investigators; for example he assumes constant wavelength within the dielectric body. If this variable were substituted for the constant, it would make his equations almost hopelessly complex.

A great deal of the known information on dielectric antennas has been assembled by McKinney[12] in a dissertation presented to the University of Texas in June, 1950. He reported also a very substantial amount of experimental data, as well as a slightly different method of attempted calculation of the fields. The method presented is also based on Schelkunoff's Equivalence Theorems, but uses an extension devised by Horton, in which he computes fictitious electric and magnetic current sheets about the dielectric which are a useful aid in the analysis. Then he obtains the vector potentials at a point in space due to these sheets and computes the E and H fields at the point. In his calculations he neglects the radiation from the end of the rod, neglects reflections in the rod, and neglects any changes which might occur to the wavelength of the wave within the dielectric. McKinney's experimental data agreed with his theoretical calculations quite closely. For the sizes and shapes used and for the $TM_{01}$ mode, it appears that his solutions are quite precise. However, his report does not show any calculations of patterns for dielectric antennas excited in the dominant mode, which is the mode most

commonly used, nor does his theory contain a precise statement of the optimum gains which may be obtained. The $TM_{01}$ mode gives a null on axis, which is unacceptable for most cases where dielectric antennas are required.

It should be pointed out that no theoretical treatment of any dielectric antennas other than those of circular cross section have been found in any of the literature. As will be brought out later in this essay, an attempt at a straightforward solution to the rectangular shaped antenna by any of the classical methods would lead to exceedingly complex equations whose solutions would involve serious difficulties. Nevertheless, in a great many applications, the rectangular antenna is the one preferred due to the predominant use of rectangular wave guide which assures no rotation of the plane of polarization. Hence this essay includes experimental gains obtained for both rectangular and circular cross section guides, including such correlation to existing theories as are possible.

# CHAPTER 1.

## REVIEW OF BASIC LAWS OF ELECTROMAGNETIC RADIATION

The objective of Chapter 1 is to develop the equations for the propagation of electromagnetic waves in a circular dielectric rod, infinitely long, imbedded in a homogeneous medium. The starting point will be Maxwell's equations. The development will be carried out for the cylindrical case because treatments of this are available in the literature. Throughout this work the MKS system of units will be used.

It has been pointed out in the introduction that Maxwell's equations hold with certainty only for macroscopic phenomena. Accordingly, we make the assumption throughout Chapters 1 and 2 that only macroscopic conditions are considered, that the media considered are isotropic and homogeneous, and that, except for stated discontinuities, the physical properties in the neighborhood of every point are continuous. Under these conditions, the following Maxwell's equations have been firmly established.

$$(1) \qquad \nabla \times E + \frac{\partial B}{\partial t} = 0$$

(2) $$\nabla \times H - \frac{\partial D}{\partial t} = J$$

where the vector quantities E, B, H, D and J are respectively the electric intensity, the magnetic induction, the magnetic intensity, the electric displacement and the current density.

Since the divergence of the curl of any vector is identically zero, we obtain by taking the divergence of (1)

(3) $$\nabla \cdot \frac{\partial B}{\partial t} = 0$$

and under the condition of continuity imposed above

(4) $$\frac{\partial}{\partial t} \nabla \cdot B = 0$$

Since the divergence of the magnetic intensity does not change with time, and certainly at some time it did not exist, it follows that

(5) $$\nabla \cdot B = 0$$

Likewise, taking the divergence of (2) and commuting the partial and del signs

(6) $$\nabla \cdot J + \frac{\partial}{\partial t} \nabla \cdot D = 0$$

Now if we denote the charge density at any point by $\rho$, the equation of continuity or the conservation of charge states that the time rate of change of $\rho$ plus the divergence of the current density is identically zero, or

$$(7) \quad \nabla \cdot J + \frac{\partial \rho}{\partial t} = 0$$

Substituting for $\nabla \cdot J$ in (6)

$$(8) \quad \frac{\partial}{\partial t} \nabla \cdot D - \frac{\partial \rho}{\partial t} = 0$$

or

$$(9) \quad \frac{\partial}{\partial t} \left( \nabla \cdot D - \rho \right) = 0$$

Applying again the argument that if the time rate of change of the quantity is zero, the quantity itself must be zero if it ever has vanished, it follows that

$$(10) \quad \nabla \cdot D = \rho$$

This tells us that the charges distributed with the density $\rho$ constitute the sources of the vector D.

Electric and Magnetic Polarization

In order to describe the electromagnetic state of a substance, it is convenient to define two

additional vectors, the electric and the magnetic polarization vectors. By definition

$$(11) \quad P = D - \varepsilon_0 E$$

$$(12) \quad M = \frac{1}{\mu_0} B - H$$

where $\varepsilon_0$ is the inductive capacity in free space and $\mu_0$ is the permeability of free space. Therefore in free space, the polarization vectors vanish.

Substituting the values for D and H from (11) and (12) into (2) and (10), we obtain the following

$$(13) \quad \nabla \times B - \mu_0 \varepsilon_0 \frac{\partial E}{\partial t} = \mu_0 \left( J + \frac{\partial P}{\partial t} + \nabla \times M \right)$$

$$(14) \quad \nabla \cdot E = \frac{1}{\varepsilon_0} ( \rho - \nabla \cdot P )$$

In any physical media which is isotropic and in which the field vectors are linear, the Electric Displacement and the Magnetic Induction are related to the corresponding field intensity by the constants of the medium

$$(15) \quad D = \varepsilon E$$

(16) $B = \mu H$

From the above equations (13-14) it is possible to account for material bodies in an electromagnetic field by an equivalent charge of density $-\nabla \cdot P$ and an equivalent distribution of current density $\frac{\partial P}{\partial t} + \nabla \times M$

It is convenient at this point to define two additional coefficients of proportionality. The electric and magnetic susceptibilities of any media, excluding ferromagnetic matérial, will be denoted by $\chi_e$ and $\chi_m$ and are defined by

(17) $P = \chi_e \varepsilon_o E$

(18) $M = \chi_m H$

We can define these scalar quantities in this way, since in isotropic media, the polarization vectors are parallel and proportional to the corresponding field vectors.

It is also convenient to define the relative dielectric constant

(19) $\epsilon = \frac{\varepsilon}{\varepsilon_o}$

and the relative permeability

(20) $K_m = \frac{\mu}{\mu_o}$

From (11), (15), (17), and (19) it follows that

(21) $\chi_e = \epsilon - 1$

and from (12), (16), (18), and (20) that

(22) $\chi_m = K_m - 1$

Vector and Scalar Potentials

To facilitate the analysis of electromagnetic fields it is useful to define some auxiliary functions called potentials. These may be shown as follows:

Equation (5) shows that the divergence of the Magnetic Induction Vector, B, is zero at all times. According to this, the field of B is always solenoidal, and therefore B can be represented as the curl of another vector A.

(23) $B = \nabla \times A$

Substituting this value of B into equation (1) gives

(24) $\nabla \times \left(E + \frac{\partial A}{\partial t}\right) = 0$

Thus the field of the vector $(E + \frac{\partial A}{\partial t})$ is irrotational and equal to the gradient of a scalar

function which we may call $\phi$.

$$(25) \quad E + \frac{\partial A}{\partial t} = -\nabla \phi \qquad \text{or} \qquad E = -\nabla\phi - \frac{\partial A}{\partial t}$$

The function A is called the vector potential of the field, and the $\phi$ is the scalar potential.

It should be noted, however, that the vector A and the scalar $\phi$ are not unique. Thus B could have been represented by the curl of another vector

$$(26) \qquad B = \nabla \times A_0$$

where

$$(27) \qquad A = A_0 - \nabla \psi$$

where $\psi$ is any arbitrary scalar function of position, It would similarly follow that

$$(28) \qquad E = -\nabla \phi_0 - \frac{\partial A_0}{\partial t}$$

and $\phi$ and $\phi_0$ would be related by

$$(29) \qquad \phi = \phi_0 + \frac{\partial \psi}{\partial t}$$

Likewise an infinite number of potentials describing the same field could be derived in the same manner.

By the definition of $\mathcal{E}$, equations (15), and using the above defined potential, equation (25),

$$(30) \qquad D = -\varepsilon\left(\nabla\phi + \frac{\partial A}{\partial t}\right)$$

And by equations (16) and (23)

$$(31) \qquad H = \frac{1}{\mu}\nabla \times A$$

Substituting (30) and (31) into equation (2)

$$\nabla \times \left(\frac{1}{\mu}\nabla \times A\right) - \frac{\partial}{\partial t}\left[-\varepsilon\left(\nabla\phi + \frac{\partial A}{\partial t}\right)\right] = J$$

and multiplying the above by $\mu$ and commuting $\frac{\partial}{\partial t}$ with $\nabla$ gives

$$(32) \quad \nabla \times \nabla \times A + \mu\varepsilon\nabla\frac{\partial\phi}{\partial t} + \mu\varepsilon\frac{\partial^2 A}{\partial t^2} = \mu J$$

By substituting (30) into equation (10) and dividing by $-\varepsilon$

$$(33) \quad \nabla \cdot \nabla\phi + \nabla \cdot \frac{\partial A}{\partial t} = -\frac{1}{\varepsilon}\rho$$

Now all particular solutions of (32) and (33) lead to the same electromagnetic field when subjected to the same boundary conditions. They differ among themselves only by the arbitrary function $\psi$. In order to specify the functions more precisely, the condition may be imposed that A and $\phi$ also satisfy

$$(34) \quad \nabla \cdot A + \mu \varepsilon \frac{\partial \phi}{\partial t} = 0$$

In order to do this, it is necessary that $\psi$ satisfy

$$(35) \quad \nabla^2 \psi - \mu \varepsilon \frac{\partial^2 \psi}{\partial t^2} = \nabla \cdot A_o + \mu \varepsilon \frac{\partial \phi_o}{\partial t}$$

Where $A_o$ and $\phi_o$ are particular solutions of (32) and (33).

The potentials A and $\phi$ by the aid of the above are completely specified. They are solutions of the following equations, which are the same as (32) and (33) except for the substitution of $\nabla \cdot A = -\mu \varepsilon \frac{\partial \phi}{\partial t}$ from (34).

$$(36) \quad \nabla \times \nabla \times A - \nabla \nabla \cdot A + \mu \varepsilon \frac{\partial^2 A}{\partial t^2} = \mu J$$

$$(37) \quad \nabla^2 \phi - \mu \varepsilon \frac{\partial^2 \phi}{\partial t^2} = -\frac{1}{\varepsilon} \rho$$

By use of the vector identity

$$(38) \quad \nabla \times \nabla \times A = \nabla \nabla \cdot A - \nabla \cdot \nabla A$$

equation (36) reduces to

$$(39) \quad \nabla^2 A - \mu \varepsilon \frac{\partial^2 A}{\partial t^2} = -\mu J$$

The relations (23) and (25) for the vectors B and E are not general. To them may be added any particular solution of the homogeneous equations:

$$(40)\qquad \nabla \times E + \frac{\partial B}{\partial t} = 0$$

$$(41)\qquad \nabla \times H - \frac{\partial D}{\partial t} = 0$$

$$(42)\qquad \nabla \cdot B = 0$$

$$(43)\qquad \nabla \cdot D = 0$$

From the symmetry of this system ~~it~~ it is evident that it can be satisfied identically by

$$(44)\qquad D = -\nabla \times A^*$$

$$(45)\qquad H = -\nabla \phi^* - \frac{\partial A^*}{\partial t}$$

from which may be obtained

$$(46)\qquad E = -\frac{1}{\varepsilon}\nabla \times A^*$$

$$(47)\qquad B = -\mu\left(\nabla \phi^* + \frac{\partial A^*}{\partial t}\right)$$

But the new potentials, $A^*$ and $\phi^*$, must be subject to the conditions

(48) $$\nabla^2 A^* - \mu\varepsilon \frac{\partial^2 A^*}{\partial t^2} = 0$$

(49) $$\nabla^2 \phi^* - \mu\varepsilon \frac{\partial^2 \phi^*}{\partial t^2} = 0$$

(50) $$\nabla \cdot A^* + \mu\varepsilon \frac{\partial \phi^*}{\partial t} = 0$$

A general solution of the inhomogeneous system given by equations (1), (2), (5) and (10) is, then

(51) $$B = \nabla \times A - \mu \frac{\partial A^*}{\partial t} - \mu \nabla \phi^*$$

(52) $$E = -\nabla \phi - \frac{\partial A}{\partial t} - \frac{1}{\varepsilon} \nabla \times A^*$$

The functions $A^*$ and $\phi^*$ are potentials of a source distribution entirely external to the region considered. Usually $A^*$ and $\phi^*$ are set equal to zero, and the potentials of all charges, wherever the source, are represented by $A$ and $\phi$.

At any point where the charge and current

densities are zero, a possible combination of potentials is $A_o = 0$ and $\phi_o = 0$. The function $\psi$ is then according to (35) any solution of the homogeneous equation

$$(53) \qquad \nabla^2\psi - \mu\varepsilon \frac{\partial^2\psi}{\partial t^2} = 0$$

Since $\phi_o = 0$ satisfies this same equation at this point, $\psi$ may be chosen in such a way that $\phi$ vanishes. In this case the field can be expressed in terms of only the vector potential. Equations (23) and (25) become

$$(54) \qquad B = \nabla \times A$$

$$(55) \qquad E = -\frac{\partial A}{\partial t}$$

and (39) and (34) become

$$(56) \qquad \nabla^2 A - \mu\varepsilon \frac{\partial^2 A}{\partial t^2} = 0$$

$$(57) \qquad \nabla \cdot A = 0$$

The foregoing paragraphs have shown how an electromagnetic field in a homogeneous medium may be reduced to a vector and a scalar potential which will satisfy Maxwell's equations.

Hertz Vectors or Polarization Potentials

It is possible under ordinary conditions to define an electromagnetic field in a homogeneous medium by means of a vector function alone.

Considering at first, no free charges or conduction currents within the medium, the field equations reduce to the homogeneous form (equations (40) through (43) ). Assume a vector, II, whose time derivative is proportional to the vector potential A

$$(58) \qquad A = \mu\varepsilon \frac{\partial \Pi}{\partial t}$$

and substitute in (23) and (25)

$$(59) \qquad B = \mu\varepsilon \, \nabla \times \frac{\partial \Pi}{\partial t}$$

$$(60) \qquad E = -\nabla\phi - \mu\varepsilon \frac{\partial^2 \Pi}{\partial t^2}$$

Using the relations $B = \mu H$ and $D = \varepsilon E$, substitute the above values in the homogeneous equation (41). After commuting the $\frac{\partial}{\partial t}$ and $\nabla$ signs, the result is

$$(61) \qquad \frac{\partial}{\partial t}\left(\nabla \times \nabla \times \Pi + \nabla\phi + \mu\varepsilon \frac{\partial^2 \Pi}{\partial t^2}\right) = 0$$

Since the scalar function $\phi$ is arbitrary as long as it satisfies equation (34), it may now be chosen to also satisfy

$$(62) \qquad \phi = -\nabla\cdot\Pi$$

If the above chosen value of $\phi$ is substituted in equation (61) and the result integrated with respect to time, the following is obtained

$$(63) \quad \nabla\times\nabla\times\Pi - \nabla\nabla\cdot\Pi + \mu\varepsilon\frac{\partial^2\Pi}{\partial t^2} = \text{a constant}$$

The value of the constant does not affect the determination of the field, and so it may be replaced by zero. Every solution of the vector equation

$$(64) \quad \nabla\times\nabla\times\Pi - \nabla\nabla\cdot\Pi + \mu\varepsilon\frac{\partial^2\Pi}{\partial t^2} = 0$$

determined an electric field through

$$(65) \qquad B = \mu\varepsilon\,\nabla\times\frac{\partial\Pi}{\partial t}$$

and

$$(66) \qquad E = \nabla\nabla\cdot\Pi - \mu\varepsilon\frac{\partial^2\Pi}{\partial t^2}$$

Equation (65) is identical to (59) and (66) is the

same as (60) with the substitution of $\nabla\nabla\cdot\Pi$ for its equal $-\nabla\phi$ by virtue of (62).

Applying the vector identity, equation (38), to equation (64) gives

$$(67) \quad \nabla\cdot\nabla\Pi - \mu\epsilon\frac{\partial^2\Pi}{\partial t^2} = 0$$

The requirement that $\phi$ satisfy equation (53) is met in equation (64) and (67).

Inasmuch as the Electric Displacement Vector, D, as well as the Magnetic Induction is solenoidal in a charge free region, an alternative solution could be similarly constructed of the form

$$(68) \quad A^* = \mu\epsilon\frac{\partial\Pi^*}{\partial t}$$

$$(69) \quad \phi^* = -\nabla\cdot\Pi^*$$

$$(70) \quad D = -\mu\epsilon\nabla\times\frac{\partial\Pi^*}{\partial t}$$

$$(71) \quad H = \nabla\nabla\cdot\Pi^* - \mu\epsilon\frac{\partial^2\Pi^*}{\partial t^2}$$

where $\Pi^*$ is any solution of (64) or (67).

It therefore follows that the electromagnetic field throughout a homogeneous isotropic region in which no charge nor current exist could be resolved into two partial fields, one derived from the vector $\Pi$ and the other from $\Pi^*$. The source of these fields is exterior to the region. In order to show the physical significance of the Hertz vectors it is necessary to relate them to their sources. This may be done by finding inhomogeneous equations from which (67) is derived.

The vector D may be expressed in terms of the electric field intensity and the electric polarization vectors, using equation (11), as $D = \mathcal{E}_0 E + P$. Then substitute this in the homogeneous field equation. Equation (41) becomes

$$(72) \qquad \nabla \times H - \mathcal{E}_0 \frac{\partial E}{\partial t} = \frac{\partial P}{\partial t}$$

and (43) becomes

$$(73) \qquad \nabla \cdot E = -\frac{1}{\mathcal{E}_0} \nabla \cdot P$$

The above two equations as well as (40) and (42) are still identically satisfied by (65) and (66), provided $\mathcal{E}$ is replaced by $\mathcal{E}_0$ and that $\Pi$ is now any

solution of

$$(74) \quad \nabla \cdot \nabla \Pi - \mu \varepsilon_0 \frac{\partial^2 \Pi}{\partial t^2} = -\frac{1}{\varepsilon_0} P$$

The source of the vector II and the electromagnetic field which it prescribes is a distribution of electric polarization P.

The vector P is the electric dipole moment per unit volume of the medium. The vector II is associated with a distribution of electric dipoles and may be called the electric polarization potential.

Similarly the field associated with $II^*$ is established by a distribution of magnetic polarization. The magnetic induction vector, B, is related to the magnetic field intensity, H, according to equations (12), by $B = \mu_0 (H + M)$. Substituting this into (40) and (42) gives

$$(75) \quad \nabla \times E + \mu_0 \frac{\partial H}{\partial t} = -\mu_0 \frac{\partial M}{\partial t}$$

and

$$(76) \quad \nabla \cdot H = - \nabla \cdot M$$

If it is further stipulated that $II^*$ shall be a solution of

$$(77) \quad \nabla \cdot \nabla \Pi^* - \mu_0 \varepsilon \frac{\partial^2 \Pi^*}{\partial t^2} = -M$$

and that $\mu_0$ replace $\mu$ in equations (70) and (71), then equations (75), (76), (41) and (43) are identically satisfied by (70) and (71).

The electric polarization P may be induced in the dielectric by the field E, but it may also contain a part whose magnitude is governed by entirely external conditions. Insofar as dielectric antennas are concerned, only the independent part, $P_0$, is of interest, which represents the electric moment of dipole oscillation activated by external power sources. This is also true of magnetic polarization. To represent these conditions, equations (11) and (12), expressed in modified form are

$$(78) \qquad E = \frac{1}{\varepsilon}(D - P_0)$$

$$(79) \qquad H = \frac{1}{\mu} B - M_0$$

in which $P_0$ and $M_0$ are prescribed and independent of E and H and where the induced polarizations of the medium have been absorbed into the parameters $\varepsilon$ and $\mu$. The electromagnetic field due to these distributions of $P_0$ and $M_0$ are given by

$$(80) \qquad E = \nabla \nabla \cdot \Pi - \mu \varepsilon \frac{\partial^2 \Pi}{\partial t^2} - \mu \nabla \times \frac{\partial \Pi^*}{\partial t}$$

$$(81) \qquad H = \varepsilon \nabla \times \frac{\partial \Pi}{\partial t} + \nabla \nabla \cdot \Pi^* - \mu \varepsilon \frac{\partial^2 \Pi^*}{\partial t^2}$$

Equation (80) above was formed, by substituting in equation (78) the value of D given by (70) and $P_o$ given by (74), replacing $\mu_o$ and $\varepsilon_o$ by $\mu$ and $\varepsilon$. Equation (81) was formed by substituting into (79) the value of B given by (65) and $M_o$ from (77). For these equations to be valid, however, it must also be stipulated that II and II* be solutions of equations corresponding to (74)

$$(82) \qquad \nabla \cdot \nabla \Pi - \mu \varepsilon \frac{\partial^2 \Pi}{\partial t^2} = -\frac{1}{\varepsilon} P_o$$

$$(83) \qquad \nabla \cdot \nabla \Pi^* - \mu \varepsilon \frac{\partial^2 \Pi^*}{\partial t^2} = -M_o$$

Using the vector identity, equation (38), and substituting (83), it ~~is~~ also possible to write (81) as

(84) $$H = \mathcal{E} \nabla \times \frac{\partial \Pi}{\partial t} + \nabla \times \nabla \times \Pi^{*} - M_0$$

The last relation shows that, since B = $\nabla \times A$, the vector potential A can be derived from the Hertzian vectors by setting

(85) $$A = \mu \mathcal{E} \frac{\partial \Pi}{\partial t} + \mu \nabla \times \Pi^{*} - \nabla \psi$$

The associated scalar potential function is

(86) $$\phi = - \nabla \cdot \Pi + \frac{\partial \psi}{\partial t}$$

in which $\psi$ must also satisfy

(87) $$\nabla^2 \psi - \mu \mathcal{E} \frac{\partial^2 \psi}{\partial t^2} = 0$$

<u>Boundary Conditions - Discontinuities in the Field Vectors</u>

The above equations have all been based upon the assumption of continuous and isotropic media. It is now necessary to consider the relations which arise due to the boundaries between two media, where there occur abrupt differences in the inductive capacities, $\mu$ and $\mathcal{E}$, and in the conductivity, $\sigma$.

To aid in the analysis, it is useful to postulate a very thin transition layer, S, between the media,

wherein the parameters $\mu$, $\mathcal{E}$ , and $\sigma$, vary rapidly but continuously from medium 1 to medium 2. Within this layer, S, the field vectors and their first derivatives are continuous, bounded functions of time and space. Consider a small right cylinder, Figure 1, in the layer such that its end surfaces lie in the surfaces of the layer and separated by a length $\Delta \ell$ .

From the volume integral of equation (5) and the divergence theorem of vector analysis[19], it follows that

$$(88) \quad \int_v \nabla \cdot B \, dv = \int_a B \cdot n \, da = 0$$

where the second integral is a surface integral over the walls and the ends of the cylinder, $\bar{n}$ being the unit vector normal to $S$ . If the elemental area of the end of the cylinder is sufficiently small, B may be considered to have a constant value over the end. Neglecting differentials of higher order, (88) may be approximated by

$$(89) \quad (B \cdot n_1 + B \cdot n_2) \Delta a + \text{contribution of walls} = 0$$

Fig. 1

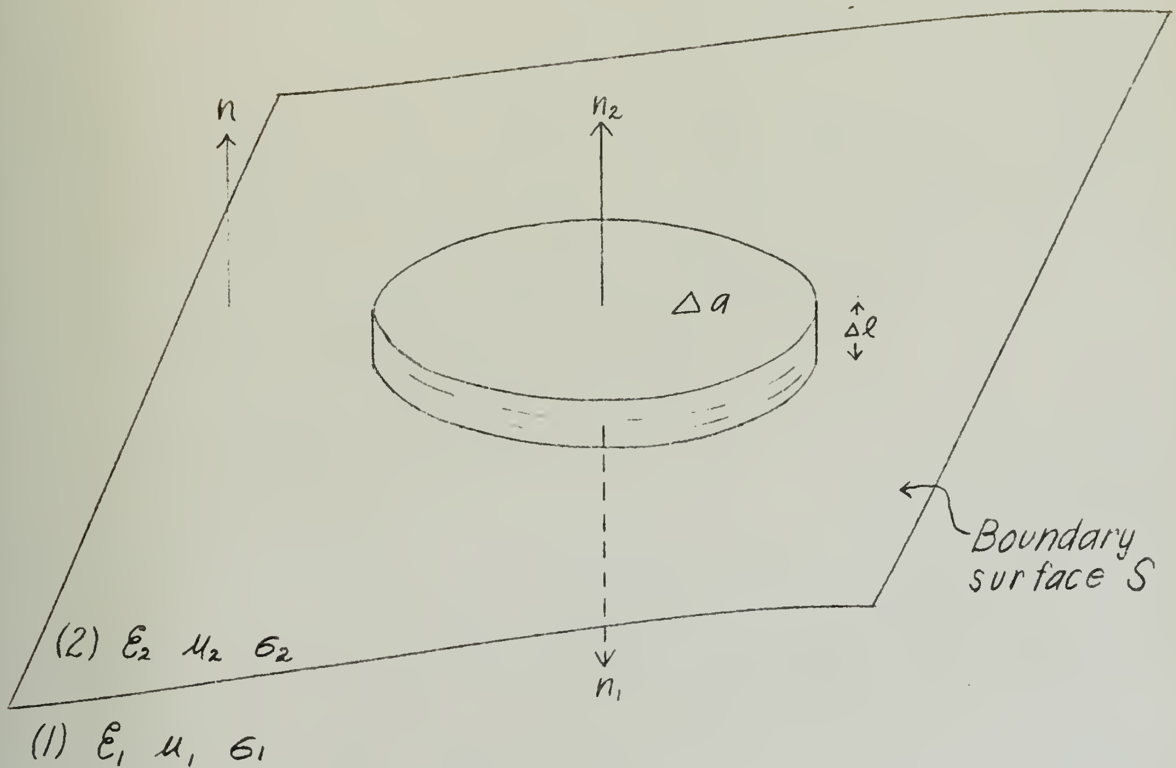


Normal Boundary Condition

where $n_1$ is unit vector normal to the surface in the sense inward to medium 1, and $n_2$ the unit vector normal in the sense inward to medium 2. Since the contribution of the walls is proportional to $\Delta \ell$, it will become vanishingly small when the limit is taken $\Delta \ell \to 0$, and the transition layer shrinks to the surface S. Designating the value of magnetic induction at the point on S in medium 1 as $B_1$, and in medium 2 as $B_2$, and passing to the limit $\Delta \ell \to 0$ and $\Delta a \to 0$

$$(90) \qquad (B_2 - B_1) \cdot n = 0$$

Thus the transition of the normal component of B across any surface of discontinuity in the medium is continuous.

Applying the same process of reasoning to the electric displacement vector D, equation (10) is integrated over a volume and its equivalent from the divergence theorem substituted. In this case, however, since $\nabla \cdot D$ is equal to the charge density, $\rho$, when it is integrated over a volume it becomes equal to the total charge within the volume, q, thus

$$(91) \qquad \int_v \nabla \cdot D \, dv = \int_a D \cdot n \, da = q$$

This charge, q, is distributed throughout the transition layer with a density $\rho$, and as the cylinder is reduced toward the limit, the q must remain the same because of the conservation of charge. Thus

$$(92) \qquad q = \rho \,\Delta \ell \,\Delta a$$

As $\Delta \ell \to 0$, $\rho$ must then $\to \infty$. It is then convenient to replace the product, $\rho \Delta \ell$, by a surface density or charge per unit area, $\omega$. The transition of the normal component of the electric displacement vector, D, across any surface, S, is then given by

$$(93) \qquad (D_2 - D_1) \cdot n = \omega$$

The presence of a layer of charge on S results in an abrupt change in the normal component of D, the amount of the discontinuity being equal to the surface density in coulombs per square meter.

It is also necessary to investigate the behavior of the tangential components of E and H at the boundary. To aid this analysis, consider a rectangle of length $\Delta S$ and thickness $\Delta \ell$, instead of a cylinder, lying at the surfaces of the two adjoining media. Let $S_0$ be the area of this

rectangle and $C_0$ be its closed contour.

Taking equation (1) and integrating over the surface

$$(94) \quad \int_{S_0} (\nabla \times E) \cdot n_0 \, da + \int_{S_0} \frac{\partial B}{\partial t} \cdot n \, da = 0$$

where $n_0$ is the unit normal vector in the conventional positive sense, as shown in Figure 2. By Stokes theorem[19], this first surface integral is equal to a line integral of the vector E about a closed contour enclosing the surface. Thus (94) may be expressed as

$$(95) \quad \int_{C_0} E \cdot ds + \int_{S_0} \frac{\partial B}{\partial t} \cdot n_0 \, da = 0$$

Designate by $\tau_1$ and $\tau_2$ the unit vectors in the direction of circulation as shown in Figure 2. Then, neglecting higher order differentials, equation (95) may be expressed by

$$(96) \quad (E \cdot \tau_1 + E \cdot \tau_2) \Delta s + \text{contribution from ends} = -\frac{\partial B}{\partial t} \cdot n_0 \Delta s \Delta l$$

Fig. 2

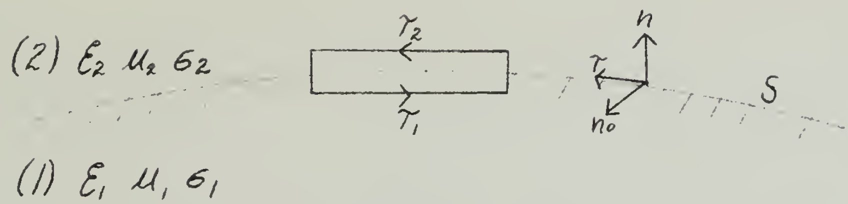


Tangential Boundary Condition

But the contributions from the ends are proportional to $\Delta \ell$ which becomes vanishingly small when the limit is taken. Let $n$ be the unit vector normal to S as shown, and $\tau$ be the unit tangent vector such that

$$(97) \qquad \tau = n_0 \times n$$

Also, it is a vector identity that

$$(98) \qquad n_0 \times n \cdot E = n_0 \cdot n \times E$$

Thus, when the limit is taken $\Delta \ell \to 0$ , $\Delta S \to 0$

$$(99) \qquad n_0 \cdot \left[ n \times \left( E_2 - E_1 \right) + \lim_{\Delta \ell \to 0} \left( \frac{\partial B}{\partial t} \Delta \ell \right) \right] = 0$$

Since $n_0 \neq 0$ and the orientation of the rectangle is arbitrary, the bracketed expression above must be zero, and so

$$(100) \qquad n \times \left( E_2 - E_1 \right) = - \lim_{\Delta \ell \to 0} \frac{\partial B}{\partial t} \Delta \ell$$

And since we have imposed the conditions that the field vectors and their derivatives be bounded, the right side of the above equation vanishes when $\Delta \ell \to 0$ Therefore

$$(101) \qquad n \times \left( E_2 - E_1 \right) = 0$$

and it is seen that the tangential components of the vector E through a surface of discontinuity are continuous.

The behavior of the magnetic intensity vector, H, at the boundary can be deduced by the same process. Integrating equation (2) over the surface of the rectangle described above and applying Stokes theorem to the first term, there is obtained

$$(102) \quad \int_{C_0} H \cdot ds - \int_{S_0} \frac{\partial D}{\partial t} \cdot n_0 da = \int_{S_0} J \cdot n_0 da$$

and it similarly follows that

$$(103) \quad n \times (H_2 - H_1) = \lim_{\Delta l \to 0} \left( \frac{\partial D}{\partial t} + J \right) \Delta l$$

The limit of $\frac{\partial D}{\partial l} \Delta l$ as $\Delta l \to 0$ will vanish because D and its derivatives are bounded. But it is possible that $\lim_{\Delta l \to 0} J \Delta l$ may not vanish, because the current $I = J \cdot n_0 \Delta s \Delta l$ is squeezed into an infinitesimal layer on the surface as the sides are brought together, and $J \to \infty$. It is convenient to represent this surface current density by K, which is defined as the limit of $J \Delta l$ as $\Delta l$ approaches zero and J becomes infinite. Then

(104) $\quad n \times (H_2 - H_1) = K$

When the conductivities of the adjoining media are finite, no surface current can exist, because E is bounded and the product of $\sigma E \Delta \ell$ vanishes with $\Delta \ell$. In the analysis of dielectric antennas, this condition exists, and so (104) can be reduced to

(105) $\quad n \times (H_2 - H_1) = 0$

In the foregoing, expressions were developed for the transition of the normal components of B and D, equations (90) and (93), and for the tangential components of E and (H), equations (101) and (105). By using (15) and (16), the normal components of H and E are immediately obtained for the transition of an electromagnetic field from one medium to another.

(106) $\quad n \cdot (H_2 - \frac{\mu_1}{\mu_2} H_1) = 0$

(107) $\quad n \cdot (E_2 - \frac{\varepsilon_1}{\varepsilon_2} E_1) = \frac{\omega}{\varepsilon_2}$

and for the tangential components of D and B

$$(108) \quad n \times \left(D_2 - \frac{\varepsilon_2}{\varepsilon_1} D_1\right) = 0$$

$$(109) \quad n \times \left(B_2 - \frac{\mu_2}{\mu_1} B_1\right) = 0$$

(for finite $\sigma$)

Poynting's Theorem in regions free of Hysteresis

Poynting's theorem gives the relation between the rate of change of energy stored in a field and the energy flow. This may be obtained as a general integral of the field equations (1), (2), (5), and (10). Since $E \cdot J$ has the dimensions of power expended per unit volume, it is apparent that this may be obtained by a scalar multiplication of (2) by E. Thus

$$(110) \quad E \cdot \nabla \times H - E \cdot \frac{\partial D}{\partial t} = E \cdot J$$

Likewise equation (1) can be given the units of power per unit volume by multiplying it by H, Thus

$$(111) \quad H \cdot \nabla \times E + H \cdot \frac{\partial B}{\partial t} = 0$$

Subtracting the above two equations

$$(112)\quad H\cdot\nabla\times E - E\cdot\nabla\times H + E\cdot\frac{\partial D}{\partial t} + H\cdot\frac{\partial B}{\partial t} = -E\cdot J$$

But, by vector identity, the first two terms of (112) are equal to $\nabla\cdot(E\times H)$ and so this equation may be written as

$$(113)\quad \nabla\cdot(E\times H) + E\cdot J = -E\cdot\frac{\partial D}{\partial t} - H\cdot\frac{\partial B}{\partial t}$$

Integrating over a volume V bounded by a surface S, and applying the divergence theorem to the first term, this becomes

$$(114)\quad \int_S (E\times H)\cdot n\,da + \int_V E\cdot J\,dv = -\int_V \left(E\cdot\frac{\partial D}{\partial t} + H\cdot\frac{\partial B}{\partial t}\right)dv$$

The terms on the right above represent the rate of decrease of the electric and magnetic energy stored in the volume. The second term on the left expresses the sum of the losses in Joule heat and the power expended by the flow of charge against the impressed forces. If there are no transformations of electromagnetic energy into elastic energy of a stressed medium, the balance is maintained by a flow

of electromagnetic energy across the surface bounding the volume. This is Poynting's interpretation of the significance of the surface integral in (114). The reduction of electromagnetic energy stored in the volume is partly accounted for by the Joule heat loss, partly by the energy introduced by the impressed forces, and the remainder flows outward across the bounding surface S, which is represented by

$$(115) \quad \int_S S \cdot n \, da = \int_S (E \times H) \cdot n \, da$$

Now the Poynting Vector is defined by

$$(116) \qquad S = E \times H \qquad \text{watts/meter}^2$$

which may be interpreted as the intensity of energy flow at a point in the field, or in other words, the energy per unit time crossing a unit area whose normal is oriented in the direction of the vector $E \times H$. It is Poynting's theorem that the vector product (116) at any point is a measure of the rate of energy flow per unit area at that point.

Another useful form of Poynting's theorem is the differential form, in which the Joule heat dissipation is separated from the power expended

by the flow of charge against the impressed forces. While E represents the total electric field intensity, let $E'$ be the intensity of the impressed electromotive forces. Then

$$E = \frac{J}{\sigma} - E' \tag{117}$$

and

$$E \cdot J = \frac{J^2}{\sigma} - E' \cdot J \tag{118}$$

Substituting (118) into (113) and replacing D by its equal $\varepsilon E$ and B by $\mu H$, the differential form becomes

$$\nabla \cdot (E \times H) + \frac{1}{\sigma} J^2 + \frac{\partial}{\partial t}\left(\frac{\varepsilon}{2} E^2 + \frac{\mu}{2} H^2\right) = E' \cdot J \tag{119}$$

## The Complex Poynting Vector

Let h $= u + w$ represent the density of the electromagnetic energy at any instant and $\rho = \frac{1}{\sigma} J^2 - E' \cdot J$ be the power expended per unit volume in Joule heat and by the flow of charge against impressed forces. From (119) with these substitutions, the Poynting theorem from (113) can be written

$$\nabla \cdot S + \frac{\partial h}{\partial t} + Q = 0 \tag{120}$$

In a stationary field, h is independent of time and the middle term would be absent. Moreover, when the field is a simple harmonic variation of time, the time average of the energy density over a period is constant and $\overline{\frac{\partial h}{\partial t}} = 0$ , the bar over the symbol indicating an average value for a period. In the case of periodic fields, it follows that

$$\overline{\nabla \cdot S} + \overline{Q} = 0$$

(121) or

$$\int_S \bar{S} \cdot n\,da + \int_v \bar{Q}\,dv = 0$$

Now these field vectors are harmonic functions of time and can be represented in complex form with real and imaginary parts. By complex variable theory, it can be shown that the time average of the product of the real parts of two complex quantities is equal to one half the real part of the product of the first quantity times the conjugate of the second quantity. Symbolically

$$\overline{\mathcal{Re}\,(A_1) \cdot \mathcal{Re}\,(A_2)} = \frac{1}{2}\,\mathcal{Re}\,(A_1 \tilde{A}_2) \tag{122}$$

where $\tilde{A}_2$ is the complex conjugate of $A_2$.

According to the above, the mean intensity of the energy flow in a harmonic electromagnetic field is the real part of the complex vector $\frac{1}{2} E \times \tilde{H}$

$$\bar{S} = \overline{\mathcal{R}e(E) \times \mathcal{R}e(H)} \tag{123}$$

$$\bar{S} = \frac{1}{2} \mathcal{R}e(E \times \tilde{H})$$

This is the complex Poynting vector which may also be denoted by

$$S^{*} = \frac{1}{2} E \times \tilde{H} \tag{124}$$

In a plane wave the magnitude of H is $\frac{E}{\eta}$, where $\eta$ is the impedance of the medium. Therefore in engineering practice the expression

$$\text{Power} \approx \frac{1}{2} \frac{(E)^2}{\eta} \tag{125}$$

is frequently used, corresponding to the vector expression (124).

Representation of a cylindrical field by Hertz Vectors

In a homogeneous medium which is free from any fixed polarization, the Maxwell Equations (1) and (2) are satisfied by the following relations in terms of Hertz vectors

$$(126) \qquad E = \nabla \times \nabla \times \Pi - \mu \nabla \times \frac{\partial \Pi^*}{\partial t}$$

$$(127) \qquad H = \nabla \times \left( \varepsilon \frac{\partial \Pi}{\partial t} + \sigma \Pi \right) + \nabla \times \nabla \times \Pi^*$$

The first of these can be readily verified by taking equation (80), applying the vector identity (38) to the first term, and noting that $\nabla^2 \Pi - \mu \varepsilon \frac{\partial^2 \Pi}{\partial t^2} = 0$

by (67). The second one is similarly verified.

Now consider a set of coordinate surfaces, Figure 3, formed by a family of cylinders whose elements are parallel to the $z$ axis. These cylindrical surfaces need not necessarily be circular or closed. Unit vectors $i_1$ , $i_2$ , and $i_3$ are assigned as shown, $i_1$ being normal to the cylinder, $i_3$ tangent to it and parallel to the $z$ axis, and $i_2$ is tangent to the surface and perpendicular

FIGURE 3.

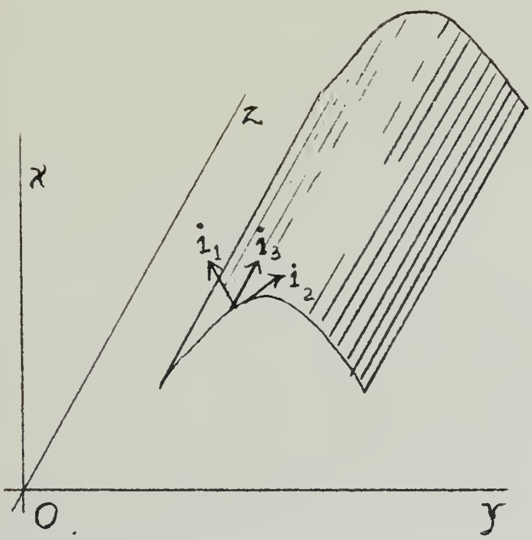


Relation of Unit Vectors to a Cylindrical Surface. The generators of the surface are parallel to the $Z$ axis.

to $i_1$ and $i_3$, forming a right handed orthogonal set. Position with respect to axes determined by the three vectors is measured by the coordinates $\mu^1, \mu^2, z$. An infinitesimal line element is

$$(128) \qquad ds = i_1 h_1 d\mu^1 + i_2 h_2 d\mu^2 + i_3 dz$$

Consider an electromagnetic field in an isotropic, homogeneous medium, unbounded in extent, existing such that the Hertz vector, II, is directed along the $z$ axis. $II_1 = 0$ $II_2 = 0$, and $II_z = \psi$. $II^* = 0$. The electric field intensity vector of this field, as given by (126) is

$$(129) \qquad E^{(1)} = \nabla \times \nabla \times \Pi$$

and the magnetic vector of the field, by (127) is

$$(130) \qquad H^{(1)} = \left(\varepsilon \frac{\partial}{\partial t} + \sigma\right) \nabla \times \Pi$$

The components of the vectors E can be calculated from (129) by means of the vector formula for the curl in an orthogonal system of curvilinear coordinates (reference 19, page 90 ), applying this twice.

(131)

$$\nabla \times F = \frac{i_1}{h_2 h_3}\left(\frac{\partial(h_3 F_3)}{\partial u_2} - \frac{\partial(h_2 F_2)}{\partial u_3}\right) + \frac{i_2}{h_3 h_1}\left(\frac{\partial(h_1 F_1)}{\partial u_3} - \frac{\partial(h_3 F_3)}{\partial u_1}\right) + \frac{i_3}{h_1 h_2}\left(\frac{\partial(h_2 F_2)}{\partial u_1} - \frac{\partial(h_1 F_1)}{\partial u_2}\right)$$

where $h_1 = \frac{ds_1}{du_1}$ $\quad h_2 = \frac{ds_2}{du_2}$ $\quad h_3 = \frac{ds_3}{du_3}$

Since $\Pi_1 = \Pi_2 = 0$ , this comes out to be, after taking the curl twice

$$E_1^{(1)} = \frac{1}{h_1}\frac{\partial^2 \Pi_z}{\partial z\, \partial u^1}$$

(132) $$E_2^{(1)} = \frac{1}{h_2}\frac{\partial^2 \Pi_z}{\partial z\, \partial u^2}$$

$$E_z^{(1)} = -\frac{1}{h_1 h_2}\left[\frac{\partial}{\partial u^1}\left(\frac{h_2}{h_1}\frac{\partial \Pi_z}{\partial u^1}\right) + \frac{\partial}{\partial u^2}\left(\frac{h_1}{h_2}\frac{\partial \Pi_z}{\partial u^2}\right)\right]$$

Likewise, to compute the components of H from (130), simply take the curl once and multiply by $\mathcal{E}\left(\frac{\partial}{\partial t} + \sigma\right)$, thus

$$H_1^{(1)} = \left(\varepsilon\frac{\partial}{\partial t} + \sigma\right)\frac{1}{h_2}\frac{\partial \Pi_z}{\partial u^2}$$

$$(133) \qquad H_2^{(1)} = -\left(\varepsilon\frac{\partial}{\partial t} + \sigma\right)\frac{1}{h_1}\frac{\partial \Pi_z}{\partial u^1}.$$

$$H_z^{(1)} = 0$$

From the $z$ scalar component of a function $\Pi_z = \psi$, an electromagnetic field has been developed which is characterized by the absence of any axial or longitudinal component of the magnetic vector. It was earlier pointed out that II is the electric polarization potential, and therefore this field may appropriately be called a field of the electric type, but following the terminology of Schelkunoff[4], it is more often referred to as the "transverse magnetic field."

It is necessary to digress to develop here the wave equation, which the function $\Pi_z = \psi$ must satisfy.

Taking the curl of equation (1) and substituting $\mu H$ for B

$$(134) \qquad \nabla \times (\nabla \times E) = -\mu\frac{\partial}{\partial t}(\nabla \times H)$$

Since $J = \sigma E$ and $D = \epsilon E$, equation (2) can be written

$$(135) \qquad \nabla \times H = \sigma E + \epsilon \frac{\partial E}{\partial t}$$

Substitute (135) into (134) and making use of the vector identity (40)

$$(136) \qquad \nabla(\nabla \cdot E) - \nabla \cdot \nabla E = -\mu\epsilon \frac{\partial^2 E}{\partial t^2} - \mu\sigma \frac{\partial E}{\partial t}$$

Rewriting equation (10), substituting $\epsilon E$ for D

$$(137) \qquad \nabla \cdot E = \frac{\rho}{\epsilon}$$

Since in free space or in any conducting medium $\rho$ is independent of the field distribution, the first term of (136) may be taken to be equal to zero. Then (136) becomes

$$(138) \qquad \nabla^2 E - \mu\epsilon \frac{\partial^2 E}{\partial t^2} - \mu\sigma \frac{\partial E}{\partial t} = 0$$

Since $J = \sigma E$, this could also be written

$$(139) \qquad \nabla^2 J - \mu\epsilon \frac{\partial^2 J}{\partial t^2} - \mu\sigma \frac{\partial J}{\partial t} = 0$$

By eliminating E from Maxwell's equations, there is also obtained

(140) $$\nabla^2 H - \mu\varepsilon \frac{\partial^2 H}{\partial t^2} - \mu\sigma \frac{\partial H}{\partial t} = 0$$

Now, returning to the equations of the cylindrical field, $\Pi_z = \psi$, the components of E and H given in (132) and (133) must satisfy the scalar wave equation

(141) $$\nabla^2 \psi - \mu\varepsilon \frac{\partial^2 \psi}{\partial t^2} - \mu\sigma \frac{\partial \psi}{\partial t} = 0$$

The Laplacian of the scalar $\psi$, expressed in general orthogonal coordinates (reference 19, page 150 ), is

(142)

$$\nabla^2\psi = \frac{1}{h_1 h_2 h_3}\left[\frac{\partial}{\partial u^1}\left(\frac{h_2 h_3}{h_1}\frac{\partial\psi}{\partial u^1}\right) + \frac{\partial}{\partial u^2}\left(\frac{h_3 h_1}{h_2}\frac{\partial\psi}{\partial u^2}\right) + \frac{\partial}{\partial u^3}\left(\frac{h_1 h_2}{h_3}\frac{\partial\psi}{\partial u^3}\right)\right]$$

Substituting this in (141), where $h_3 = 1$, $u^3 = z$

(143)

$$\frac{1}{h_1 h_2}\frac{\partial}{\partial u^1}\left(\frac{h_2}{h_1}\frac{\partial\psi}{\partial u^1}\right) + \frac{1}{h_1 h_2}\frac{\partial}{\partial u^2}\left(\frac{h_1}{h_2}\frac{\partial\psi}{\partial u^2}\right) + \frac{\partial^2\psi}{\partial z^2} - \mu\varepsilon\frac{\partial^2\psi}{\partial t^2} - \mu\sigma\frac{\partial\psi}{\partial t} = 0$$

The elementary harmonic solutions of (143) are of the form

$$\psi = f(u^1, u^2)\, e^{\pm i h z - i\omega t} \tag{144}$$

where $f(u^1, u^2)$ is a solution of

(145)

$$\frac{1}{h_1 h_2}\frac{\partial}{\partial u^1}\left(\frac{h_2}{h_1}\frac{\partial f}{\partial u^1}\right) + \frac{1}{h_1 h_2}\frac{\partial}{\partial u^2}\left(\frac{h_1}{h_2}\frac{\partial f}{\partial u^2}\right) + (k^2 - h^2) f = 0$$

Similarly, a partial field can be derived from a second Hertz vector $\Pi^*$ by the operations

$$\begin{aligned} E^{(2)} &= -\mu \frac{\partial}{\partial t} \nabla \times \Pi^* \\ H^{(2)} &= \nabla \times \nabla \times \Pi^* \end{aligned} \tag{146}$$

If the vector $\Pi^*$ is directed along the $z$ axis, the vector components come out to be

$$\begin{aligned} E_1^{(2)} &= -\frac{\mu}{h_2}\frac{\partial^2 \Pi_z^*}{\partial t\, \partial u^2} \\ E_2^{(2)} &= \frac{\mu}{h_1}\frac{\partial^2 \Pi_z^*}{\partial t\, \partial u^1} \\ E_z^{(2)} &= 0 \end{aligned} \tag{147}$$

$$H_1^{(2)} = \frac{1}{h_1} \frac{\partial^2 \Pi_z^*}{\partial z \, \partial u^1}$$

$$(148) \qquad H_2^{(2)} = \frac{1}{h_2} \frac{\partial^2 \Pi_z^*}{\partial z \, \partial u^2}$$

$$H_z^{(2)} = -\frac{1}{h_1 h_2}\left[\frac{\partial}{\partial u^1}\left(\frac{h_2}{h_1} \frac{\partial \Pi_z^*}{\partial u^1}\right) + \frac{\partial}{\partial u^2}\left(\frac{h_1}{h_2} \frac{\partial \Pi_z^*}{\partial u^2}\right)\right]$$

The scalar function $\Pi_z^*$ is a solution of (141), and is a field of the magnetic type or transverse electric, characterized by a zero longitudinal component of E.

If the partial fields derived from $\Pi_z$ and $\Pi_z^*$ are superposed, the electromagnetic fields are of such generality that they can satisfy any prescribed set of boundary conditions on any cylindrical surface whose generating elements are parallel to the Z axis. In general, the choice of the coordinates is limited practically to systems in which the variables of equation (145) are separable. It is for this reason that this development of equations of electromagnetic waves in a rod is limited to the case of the circular cylinder.

Wave Functions of the Circular Cylinder

The simplest of the separable cases is that in which the family $u^1$=constant is represented by a set of coaxial cylinders, where $u^1 = r$, $u^2 = \theta$, $h_1 = 1$ and $h_2 = r$. See Figure 4. In this case equation (145) reduces to:

(149)
$$\frac{1}{r}\frac{\partial}{\partial r}\left(r\frac{\partial f}{\partial r}\right) + \frac{1}{r^2}\frac{\partial^2 f}{\partial \theta^2} + (k^2 - h^2)f = 0$$

which can be separated by writing $f(r,\theta)$ as a product

(150) $$f = f_1(r)\, f_2(\theta)$$

where $f_1(r)$ is an arbitrary solution of the equation

(151)
$$r\frac{d}{dr}\left(r\frac{df_1}{dr}\right) + \left[(k^2 - h^2)r^2 - n^2\right]f_1 = 0$$

and $f_2(\theta)$ is an arbitrary solution of

(152) $$\frac{d^2 f_2}{d\theta^2} + n^2 f_2 = 0$$

Solutions of (151) are Bessel's functions, and a solution to (152) is $f_2(\theta) = e^{in\theta}$. The parameter, n, is a separation constant. Its choice is governed by the physical requirement that the field must be single valued at any fixed point in space. Since at the present, the discussion is limited to continuous

FIGURE 4.

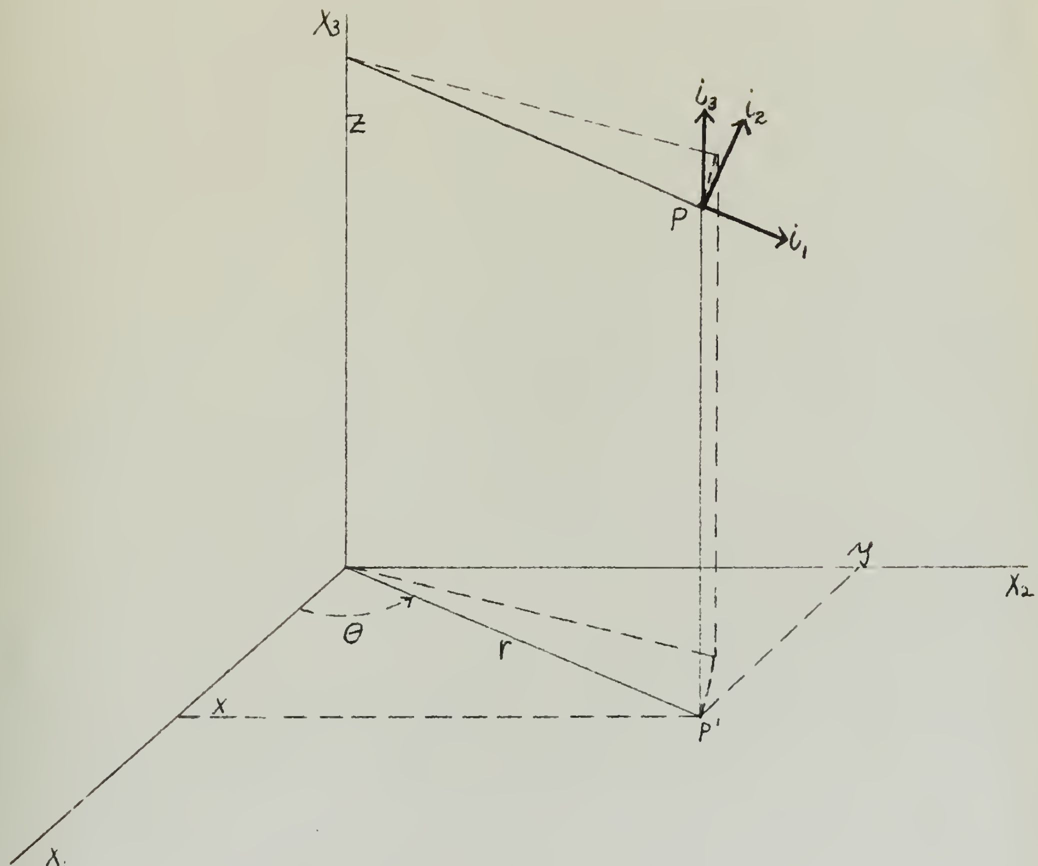


Coordinates of the Circular Cylinder

media, the field is periodic in θ and the values of n are limited to integers, 0, 1, 2, 3....., either positive or negative. However, in a field represented by particular solutions of (151) and (152), which is bounded by planes $\theta = \theta_1$, and $\theta = \theta_2$, non-integral values would in general have to be assigned to n.

The constant h is, in general, a complex quantity pertaining to the propagation of the wave and is called the propagation factor. An explicit expression for h in terms of the frequency and the constants of the medium can be obtained only after the behavior of $\psi$ over a cylinder $r =$ constant on a plane $z =$ constant has been prescribed.

The equation (151) is Bessel's equation, the solutions of which are the Bessel functions $J_n(\sqrt{k^2-h^2}\,r)$. In accordance with terminology employed by Jahnke and Emde and several other authors the term "circular cylinder function" will be used to denote any particular solution of (151) and designated by the letters $f_1 = Z_n(\sqrt{k^2-h^2}\,r)$. The order of the functions whose argument is $\sqrt{k^2-h^2}\,r$ is n. Particular solutions of the scalar wave equation (141) which are periodic in t and θ can be constructed from elementary waves of the form

(153)

$$\psi_n = e^{in\theta} Z_n\left(\sqrt{k^2-h^2}\, r\right) e^{\pm ihz - i\omega t}$$

Reference is made to standard texts in mathematics for the properties of the various Bessel functions, but it is essential to this development to note several pertinent characteristics. The Bessel function, or circular cylinder function of the first kind, is finite and converges for all finite values of the argument. For non-integral values of n it has two linearly independent solutions for $J_n(\rho)$ and $J_{-n}(\rho)$ ; but if n is an integer the two solutions are not independent. A second independent solution can be obtained by the Bessel function of the second kind, $N_n(\rho)$ , defined by

$$(154) \qquad N_n(\rho) = \frac{1}{\sin n\pi}\left[J_n(\rho)\cos n\pi - J_{-n}(\rho)\right]$$

When n is an integer, $N_n(\rho)$ is a second solution, but this is useless at $\rho = 0$, for the function becomes infinite at this point. Solutions can be obtained

in terms of still other functions, the Hankel functions, $H_n^{(1)}(\rho)$ and $H_n^{(2)}(\rho)$, which are merely linear combinations of the first and second Bessel functions as follows

$$(155) \qquad H_n^{(1)}(\rho) = J_n(\rho) + i N_n(\rho)$$

$$(156) \qquad H_n^{(2)}(\rho) = J_n(\rho) - i N_n(\rho)$$

But the Hankel functions likewise become infinite for $\rho = 0$ and so are excluded from use where the argument is very small. Expansion of the J and N functions shows a similarity to the cosine and sine functions and, as such, represent standing waves when used with the time factor $e^{-i\omega t}$. The H functions correspond to exponential functions with imaginary exponents, and, when used with the time factor $e^{-i\omega t}$ represent traveling cylindrical waves.

<u>The Field of Circularly Cylindrical Wave Functions</u>

Every electromagnetic field within a homogeneous isotropic domain can be represented by linear

combinations of the following functions

$$(157) \qquad \psi_{nhk} = e^{in\theta} J_n\left(\sqrt{k^2-h^2}\, r\right) e^{\pm ihz - i\omega t}$$

$$(158) \qquad \psi_{nhk} = e^{in\theta} H_n^{(1)}\left(\sqrt{k^2-h^2}\, r\right) e^{\pm ihz - i\omega t}$$

The first equation, (157), alone, is sufficient to represent an electromagnetic field within finite domains including the axis $r=0$. But at great distances from the source, (158) must be used, for as $\left(\sqrt{k^2-h^2}\, r\right)$ becomes very large, the function reduces to a wave travelling radially outward. This can be more readily understood when it is noted that for very large arguments $(\rho)$ the Hankel function is approximately given by

$$(159) \qquad H_n^{(1)}(\rho) = \sqrt{\frac{2}{\pi\rho}}\; e^{i\left(\rho - \frac{2n+1}{4}\pi\right)}$$

Each elementary wave is identified by the parameters n, h, k. When n is zero the field is independent of θ

and is symmetric about the axis, when h is zero the propagation is purely radial and the field becomes only two dimensional. The two functions, (157) and (158) may represent inhomogeneous plane waves as well as homogeneous. The planes of constant phase are propagated along the $z$ axis with a velocity $v = \frac{\omega}{\alpha}$ where $\alpha$ is the real part of h, but the amplitudes over these planes are functions of $r$ and θ.

The formulas for the components of the field vectors can be obtained from equations (147) and (148), remembering that $\Pi_1 = \Pi_2 = 0$ and $\Pi_z = \psi$. Also, the above equations were for a generalized cylindrical field, while we are now restricted to circularly cylindrical functions and therefore, $h_1 = h_3 = 1$, $h_2 = r$, and $u^1 = r$, $u^2 = \theta$, $z = z$. Note also that, due to the exponential, $e^{\pm ihz - i\omega t}$, differentiation with respect to $z$ multiplies the function by $\pm ih$. For the transverse magnetic field, the results are:

$$E_r^{(1)} = \pm ih\frac{\partial\psi}{\partial r}$$

$$E_\theta^{(1)} = \pm\frac{ih}{r}\frac{\partial\psi}{\partial\theta} \tag{160}$$

$$E_z^{(1)} = (k^2 - h^2)\psi$$

$$H_r^{(1)} = -\frac{ik^2}{\mu\omega}\frac{1}{r}\frac{\partial\psi}{\partial\theta}$$

(161)
$$H_\theta^{(1)} = \frac{ik^2}{\mu\omega}\frac{\partial\psi}{\partial r}.$$

$$H_z^{(1)} = 0$$

Similarly for the transverse electric field

$$E_r^{(2)} = \frac{i\mu\omega}{r}\frac{\partial\psi}{\partial\theta}$$

(162)
$$E_\theta^{(2)} = -i\mu\omega\frac{\partial\psi}{\partial r}$$

$$E_z^{(2)} = 0$$

$$H_r^{(2)} = \pm ih\frac{\partial\psi}{\partial r}$$

(163)
$$H_\theta^{(2)} = \pm\frac{ih}{r}\frac{\partial\psi}{\partial\theta}$$

$$H_z^{(2)} = (k^2-h^2)\psi$$

When initial conditions are prescribed over given plane or cylindrical surfaces, a solution can be constructed by superposing these elementary wave functions. For fixed values of $\omega$ (or $k$) and h, the field in cylindrical coordinates may be represented by the equations (164) and (165) below, in which the $a_n$ and $b_n$ coefficients must be determined from the initial conditions.

$$E_r = ih \sum_{n=-\infty}^{\infty} a_n \frac{\partial \psi_n}{\partial r} - \frac{\mu\omega}{r} \sum_{n=-\infty}^{\infty} n b_n \psi_n$$

$$(164) \qquad E_\theta = -\frac{h}{r} \sum_{n=-\infty}^{\infty} n a_n \psi_n - i\mu\omega \sum_{n=-\infty}^{\infty} b_n \frac{\partial \psi_n}{\partial r}$$

$$E_z = (k^2 - h^2) \sum_{n=-\infty}^{\infty} a_n \psi_n$$

$$H_r = \frac{k^2}{\mu\omega} \frac{1}{r} \sum_{n=-\infty}^{\infty} n a_n \psi_n + ih \sum_{n=-\infty}^{\infty} b_n \frac{\partial \psi_n}{\partial r}$$

$$(165) \qquad H_\theta = \frac{ik^2}{\mu\omega} \sum_{n=-\infty}^{\infty} a_n \frac{\partial \psi_n}{\partial r} - \frac{h}{r} \sum_{n=-\infty}^{\infty} n b_n \psi_n$$

$$H_z = (k^2 - h^2) \sum_{n=-\infty}^{\infty} b_n \psi_n$$

Propagation along a circular cylinder

Consider a circular cylinder of infinite length, of radius a, of material with propagation constant $k_1$ imbedded in an infinite homogeneous medium of propagation constant $k_2$. The field must be finite at the center and consequently the wave functions within the cylinder will be constructed of Bessel functions of the first kind. Outside the cylinder the field will extend to infinity and consequently the functions must be constructed of Hankel functions. In the equations below $\chi_1^2$ is substituted for $(k_1^2-h^2)$ and $\chi_2^2$ is substituted for $(k_2^2-h^2)$. The function $e^{in\theta+ihz+i\omega t}$ is abbreviated to Fn. Summations are in each case from $n=-\infty$ to $n=+\infty$. A prime above a cylinder function indicates differentiation with respect to the argument $(\chi r)$. The superscripts i or e over the coefficients $a_n$ and $b_n$ indicate points interior and exterior to the cylinder respectively.

$$E_r^i = \sum \left[\frac{ih}{\chi_1} J_n'(\chi_1 r)\, a_n^i - \frac{\mu_1 \omega n}{\chi_1^2 r} J_n(\chi_1 r)\, b_n^i\right] F_n$$

$$E_\theta^i = - \sum \left[\frac{nh}{\chi_1^5 r} J_n(\chi_1 r)\, a_n^i + \frac{i\mu_1\omega}{\chi_1} J_n'(\chi_1 r)\, b_n^i\right] F_n \qquad (166)$$

$$E_z^i = \sum \left[J_n(\chi_1 r)\, a_n^i\right] F_n$$

$$H_r^i = \sum \left[\frac{nk_1^2}{\mu_1\omega\chi_1^2 r} J_n(\chi_1 r)\, a_n^i + \frac{ik}{\chi_1} J_n'(\chi_1 r)\, b_n^i\right] F_n$$

(167) $$H_\theta^i = \sum \left[\frac{ik_1^2}{\mu_1\omega\chi_1} J_n'(\chi_1 r)\, a_n^i - \frac{nk}{\chi_1^2 r} J_n(\chi_1 r)\, b_n^i\right] F_n$$

$$H_z^i = \sum \left[J_n(\chi_1 r)\, b_n^i\right] F_n$$

$$E_r^e = \sum \left[\frac{ik}{\chi_2} H_n^{(1)'}(\chi_2 r)\, a_n^e - \frac{\mu_2\omega n}{\chi_2^2 r} H_n^{(1)}(\chi_2 r)\, b_n^e\right] F_n$$

(168) $$E_\theta^e = -\sum \left[\frac{nk}{\chi_2^2 r} H_n^{(1)}(\chi_2 r)\, a_n^e + \frac{i\mu_2\omega}{\chi_2} H_n^{(1)'}(\chi_2 r)\, b_n^e\right] F_n$$

$$E_z^e = \sum \left[H_n^{(1)}(\chi_2 r)\, a_n^e\right] F_n$$

$$H_r^e = \sum \left[\frac{nk_2^2}{\mu_2\omega\chi_2^2 r} H_n^{(1)}(\chi_2 r)\, a_n^e + \frac{ik}{\chi_2} H_n^{(1)'}(\chi_2 r)\, b_n^e\right] F_n$$

(169) $$H_\theta^e = \sum \left[\frac{ik_2^2}{\mu_2\omega\chi_2} H_n^{(1)'}(\chi_2 r)\, a_n^e - \frac{nk}{\chi_2^2 r} H_n^{(1)}(\chi_2^2 r)\, b_n^e\right] F_n$$

$$H_z^e = \sum \left[H_n^{(1)}(\chi_2 r)\, b_n^e\right] F_n$$

The coefficients of the expansions and the propagation factor h must next be determined. At the boundary where r is equal to the constant radius of the cylinder, a, the tangential components of the field are continuous, which condition supplies a relation between the coefficients. From the continuity of the tangential components of E, the following relations are found, where the substitutions have been made $\chi_1 a = \rho$ , $\chi_2 a = \nu$

(170)

$$\frac{nh}{\rho^2} J_n(\rho) a_n^i + \frac{i\omega\mu_1}{\rho} J_n'(\rho) b_n^i = \frac{nh}{\nu^2} H_n^{(1)}(\nu) a_n^e + \frac{i\omega\mu_2}{\nu} H_n^{(1)\prime}(\nu) b_n^e$$

(171) $$J_n(\rho) a_n^i = H_n^{(1)}(\nu) a_n^e$$

From the tangential components of H, similar relations are found as follows:

(172)

$$\frac{ik_1^2}{\mu_1\omega\rho} J_n'(\rho) a_n^i - \frac{nh}{\rho^2} J_n(\rho) b_n^i = \frac{ik_2^2}{\mu_2\omega\nu} H_n^{(1)\prime}(\nu) a_n^e - \frac{nh}{\nu^2} H_n^{(1)}(\nu) b_n^e$$

$$(173) \qquad J_n(p)\, b_n^i = H_n^{(1)}(v)\, b_n^e$$

The above relations constitute a homogeneous system of linear equations satisfied by the four coefficients $a_n^i$, $b_n^i$, $a_n^e$, $b_n^e$ . There will be a nontrivial solution only if the rank of the matrix is less than four, which will be true if its determinant is zero. The propagation factor is determined by the condition that the determinant of (170) through (173) shall vanish.

Expansion of this determinant leads to the transcendental equation

(174)

$$\left[\frac{\mu_1}{p}\frac{J_n'(p)}{J_n(p)} - \frac{\mu_2}{v}\frac{H_n^{(1)'}(v)}{H_n^{(1)}(v)}\right]\left[\frac{k_1^2}{\mu_1 p}\frac{J_n'(p)}{J_n(p)} - \frac{k_2^2}{\mu_2 v}\frac{H_n^{(1)'}(v)}{H_n^{(1)}(v)}\right] = n^2 h^2 \left(\frac{1}{v^2} - \frac{1}{p^2}\right)^2$$

The roots of (174) are the allowed values of the propagation factor, h, and so determine the characteristic or natural modes of propagation.

Thus, there has been developed an equation whose solution enables calculation of natural modes

and the propagation constants for long rods. Equation (149) expresses the true result of Maxwell in an infinitely long rod imbedded in a perfectly homogeneous medium. Equations (157) and (158) are valid solutions to this equation. By use of the continuity of the tangential components of E and H at the boundary of the rod, it was possible to use (157) and (158) to find relations which enable one to solve simultaneously for the propagation constants.

Solutions to (174) have been obtained and it has been shown[9,10] that they verify experimental results within the accuracy of experimental procedure. In the next chapter, a nomogram will be presented which provides solutions for the case of dielectric rods in air or vacuum.

It should be emphasized that the preceding development assumes that the rod is long enough to neglect boundary conditions at the ends, and that the radius, a, is not microscopic as far as the external wave is concerned. The question as to what size rod is required to justify the assumption that the radius is not microscopic is most pertinent. If the radius is small compared to a wavelength, it is probably in error to assume that Hankel functions

are required for all waves exterior to the rod while Bessel functions of the first kind suffice for internal waves.

Having obtained the propagation constants, available published literature indicates that all authors proceed to determine radiation characteristics on the assumption that the propagation is truly constant throughout the rod. The experimental evidence that this is not true in short rods of diameters of a wavelength or less has apparently been neglected, and available published theories on powers show serious defects when confronted with experimental evidence. For example, experimental curves[8,12] show that power on axis is linear with exposed length of dielectric for short antennas. The published theories do not permit such a relation.

A satisfactory solution to this problem from a theoretical standpoint cannot be completed in the present work. The experimental data presented may provide a stepping stone toward its ultimate achievement.

# CHAPTER 2.

## APPLICATION OF ELECTROMAGNETIC THEORY TO CIRCULAR DIELECTRIC RODS

In Chapter 1 an equation was developed expressing in circular coordinates the natural modes of electromagnetic waves in an infinitely long cylinder imbedded in an infinite homogeneous medium. The next step is to specialize this to the case of a dielectric cylinder imbedded in air or vacuum. Furthermore, particular solutions of (174) are desired, and to achieve this, the equations will be put in a form more suitable for use with available tables of cylinder functions.

The equation (174) may be expressed in Modified Bessel functions ($K_n$ functions) by use of the relation

$$(175) \qquad K_n(\rho) = i \frac{\pi}{2} e^{\frac{n\pi i}{2}} H_n^{(1)}(i\rho)$$

or

$$(176) \qquad H_n^{(1)}(v) = -i \frac{2}{\pi} e^{-\frac{n\pi i}{2}} K_n(-iv)$$

and

$$(177) \qquad H_n^{(1)'}(v) = -\frac{2}{\pi} e^{-\frac{n\pi i}{2}} K_n'(-iv)$$

Letting -iv = q, then

$$(178) \qquad \frac{H_n^{(1)'}(v)}{v H_n^{(1)}(v)} = -\frac{K_n'(q)}{q K_n(q)} = -g$$

We let the above expression be -g, by definition, to simplify notation. Also let

$$(179) \qquad \frac{J_n'(p)}{p J_n(p)} = f$$

Substituting these relations in (174)

(180)

$$(\mu_1 f + \mu_2 g)\left(\frac{k_1^2}{\mu_1} f + \frac{k_2^2}{\mu_2} g\right) = n^2 h^2 \left(\frac{1}{-q^2} + \frac{1}{-p^2}\right)^2$$

Since we are only concerned with dielectric rod and air or free space, we may consider

(181) $\mu_1 = \mu_2 = \mu$

The constants k and h were introduced in our elementary harmonic solutions of the scalar wave equation in a cylinder, equations (143-145). From this, k was equal $\sqrt{\omega^2\mu\varepsilon - i\omega\sigma\mu}$ , and we may now set $\sigma = 0$ , since the conductivity of dielectric and air are negligible. Thus $k_1 = \omega\sqrt{\mu\varepsilon_1}$ ,and $k_2 = \omega\sqrt{\mu\varepsilon_2}$ . In the notation introduced with equations (166-169), $\chi_1^2 = k_1^2 - h^2$ and $\chi_2^2 = k_2^2 - h^2$ , Since $\chi_1 = \frac{p}{a}$ and $\chi_2 = \frac{v}{a} = \frac{iq}{a}$, it follows that

(182)
$$h^2 + \frac{p^2}{a^2} = \omega^2\mu\varepsilon_1$$

(183)
$$h^2 - \frac{q^2}{a^2} = \omega^2\mu\varepsilon_0$$

Where the subscript on $\varepsilon_2$ has now been changed to zero to indicate the special case of free space.

Eliminating h from the above, the following is obtained

$$(184) \qquad \frac{p^2+q^2}{a^2} = \omega^2 \mu (\mathcal{E}_1 - \mathcal{E}_0)$$

Let us now set for the relative dielectric constant

$$(185) \qquad \epsilon = \frac{\mathcal{E}_1}{\mathcal{E}_0}$$

and use the relation

$$(186) \qquad c = \frac{1}{\sqrt{\mathcal{E}_0 \mu}}$$

to put equation (184) in the form

$$(187) \qquad \frac{\omega a}{c} = \frac{2\pi a}{\lambda_0} = \sqrt{\frac{p^2+q^2}{\epsilon - 1}}$$

which will be one of our principal relationships to use in solving (174) for the propagation constants.

To obtain the other principal equation, we substitute into (180) the value of h in terms of the other constants as given in equation (182), substitute for $k_1$ and $k_2$ their corresponding values as above, and substitute for $\omega$ from (187). After simplification, using (186), the result is

$$(188) \qquad (\epsilon f + g)(f + g) = n^2 \left(\frac{\epsilon}{p^2} + \frac{1}{q^2}\right)\left(\frac{1}{p^2} + \frac{1}{q^2}\right)$$

For a given n, $\omega$, and $\epsilon$, the last two equations can be solved for p and q which define the mode propagated along the rod, and enable calculation of the other constants.

From equations (182) and (183) some interesting deductions can be drawn concerning the longitudinal propagation factor, h. We note from (183) that if q is zero, that h is equal to $\omega\sqrt{\mu\epsilon_0}$ , and therefore the wave is traveling with the velocity and wavelength characteristic of free space. If p is zero, (182 ) shows that h is equal $\omega\sqrt{\mu\epsilon_1}$ , and the wave is traveling with the wavelength characteristic of the dielectric. For a given dielectric, frequency, and diameter, equation (187) shows that the sum $(p^2 + q^2)$ is a constant. It will later be shown that p is subject to less variation than q. If q is small, which is the case for small diameters, the $K_n(q)$ becomes very large compared to $J_n(p)$. Since the wave functions outside the cylinder were constructed from $H_n^{(1)}$ functions, which were later converted to $K_n$ functions, it is apparent that the energy outside the dielectric is large compared to that inside. Also for small q, the wavelength and

velocity characteristics are near that of free space. Conversely, for large diameters, q is large relative to p, and $K_n(q)$ becomes very small compared to $J_n(p)$. Thus the energy is contained mostly inside the dielectric, with a relatively thin film of energy on the outside surfaces. The wavelength in this case approaches the characteristic of the dielectric. Qualitatively, we might expect in view of this, unless the dielectric is ideal and lossless, that losses increase rapidly with increasing diameter of the rod.

An important factor needed for the design of dielectric antennas is the ratio of free space wavelength to the wavelength of propagation, or apparent index of refraction. We have noted, where conductivity is zero, that:

(a) the propagation constant, characteristic of the dielectric, $k_1$, is equal $\omega\sqrt{\mu\varepsilon_1}$

(b) the propagation constant characteristic of free space,

$$k_2 = k_0 = \omega\sqrt{\mu\varepsilon_0} = \frac{2\pi}{\lambda_0}$$

(c) the longitudinal propagation factor for the combination is

$$h = \frac{2\pi}{\lambda_1}$$

It follows that

$$(189) \qquad \frac{k}{k_2} = \frac{\lambda_0}{\lambda_1} = n_a$$

where $n_a$ is used as a symbol for the apparent index of refraction. In order to obtain an explicit expression for $n_a$ in terms of the other constants in these equations, divide equation (180) by $k_2^2$ and note that

$$\frac{k_1^2}{k_2^2} = \frac{\epsilon_1}{\epsilon_2} = \epsilon$$

Solving for $\frac{k^2}{k_1^2}$ yields

$$(190) \qquad \frac{k^2}{k_2^2} = n_a^2 = \frac{(\epsilon f + g)(f + g)}{n^2\left(\frac{1}{p^2} + \frac{1}{q^2}\right)^2}$$

Substituting for the numerator its quivalent given by (188), and extracting the square root, we have $n_a$ in terms of $\epsilon$, p, and q.

$$(191) \qquad n_a = \frac{\left(\epsilon/p^2 + 1/q^2\right)^{1/2}}{\left(1/p^2 + 1/q^2\right)^{1/2}}$$

which is in a convenient form for obtaining $n_a$ when p and q have been determined.

Curves of calculated apparent indices of refraction for various diameters and dielectric constants for the dominant mode (n = 1) are given in Figure 5. These are in reasonably close agreement with experimental values obtained by McKinney[12].

It can be readily understood that this apparent index of refraction is of fundamental importance in the design of a dielectric antenna. It has been shown[8,11,13] that the optimum length of a cylindrical dielectric rod, to maximize radiation on axis, is that length which causes the wave to emerge from the end delayed by a half period behind the external wave. This length has been shown[8,11,13] to be

(192) $$\ell_0 = \frac{\lambda_0}{2(n_a - 1)}$$

which is obtained as follows. Consider that the time for the wave phase to pass through the dielectric, $t_d$, must be greater than the time for the phase to sweep through the same distance in air, $t_a$, by one half period, $\frac{\pi}{\omega}$ .

Thus $$t_d - t_a = \frac{\ell_0}{v_1} - \frac{\ell_0}{c} = \frac{\pi}{\omega}$$

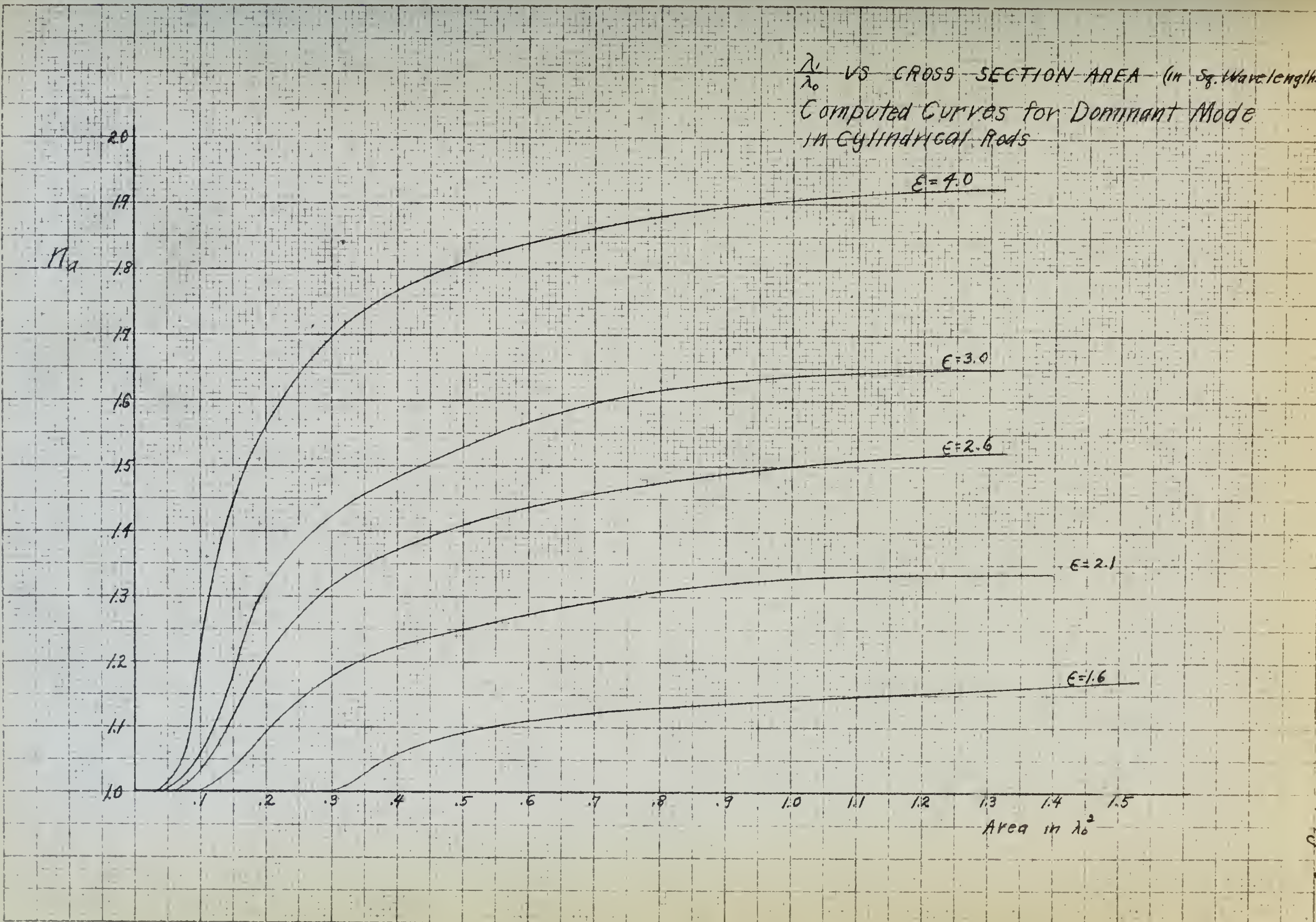

$\frac{\lambda_1}{\lambda_0}$ VS CROSS SECTION AREA (in Sq. Wavelengths)
Computed Curves for Dominant Mode in Cylindrical Rods
$\epsilon = 4.0$
$\epsilon = 3.0$
$\epsilon = 2.6$
$\epsilon = 2.1$
$\epsilon = 1.6$
$n_a$
2.0
1.9
1.8
1.7
1.6
1.5
1.4
1.3
1.2
1.1
1.0
.1
.2
.3
.4
.5
.6
.7
.8
.9
1.0
1.1
1.2
1.3
1.4
1.5
Area in $\lambda_0^2$


Fig 5

Substituting $c = \frac{\omega}{2\pi}\lambda_0$ and $v_1 = \frac{\omega}{2\pi}\lambda_1 = \frac{\omega}{2\pi}\frac{\lambda_0}{m_a}$

and solving for $\ell_0$, equation (192) is obtained. The above expression for the optimum length has been verified experimentally by several investigators[7,11].

In the discussion so far, the mode of the electromagnetic waves, which is determined by the n in the preceding equations, has not been specified and the equations hold for any mode. It was shown in Chapter 1 that, if the wave is to be periodic in $\theta$, that n must be an integer. For a practical dielectric antenna, it is necessary to specify this further. The mode normally used for propagation in the wave guide and for exciting the dielectric is the so called dominant mode, which is the mode of propagation having the lowest cut off frequency. Shelkunoff has shown[4], by allowing q to approach zero and evaluating the remaining terms in the equation, that the $n = 1$ mode has a cut off frequency which is theoretically zero. For n zero or greater than 1, it is also shown that the cut off is not zero. Therefore,

the dominant mode is $n = 1$ and this is the only mode considered for the remainder of this work.

The method of solution of equations (187) and (188) must be either numerical or graphical, and both of these methods are cumbersome and tedious. In order to facilitate obtaining rapid solutions, at a small sacrifice of precision, nomograph charts A and B have been prepared. See Figures 6 and 7.

Chart A, Figure 6, is a nomogram of the equation

$$p^2 + q^2 = \text{constant}$$

and Chart B, Figure 7, is a nomogram of

$$(\epsilon f + g)(f + g) - (\epsilon/p + 1/q)(1/p + 1/q) = 0$$

To obtain a solution, we seek values of p and q to satisfy both equations. It is assumed that the relative dielectric constant, $\epsilon$, the radius, a, and the free space wavelength, $\lambda_0$, are known. To use the accompanying charts, proceed as follows:

Calculate the constant, $p^2 + q^2$, by slide rule, from the equation (187). Thus

$$p^2 + q^2 = (\epsilon - 1)\left(\frac{2\pi a}{\lambda_0}\right)^2$$

Nomogram
CHART A

Fig 6

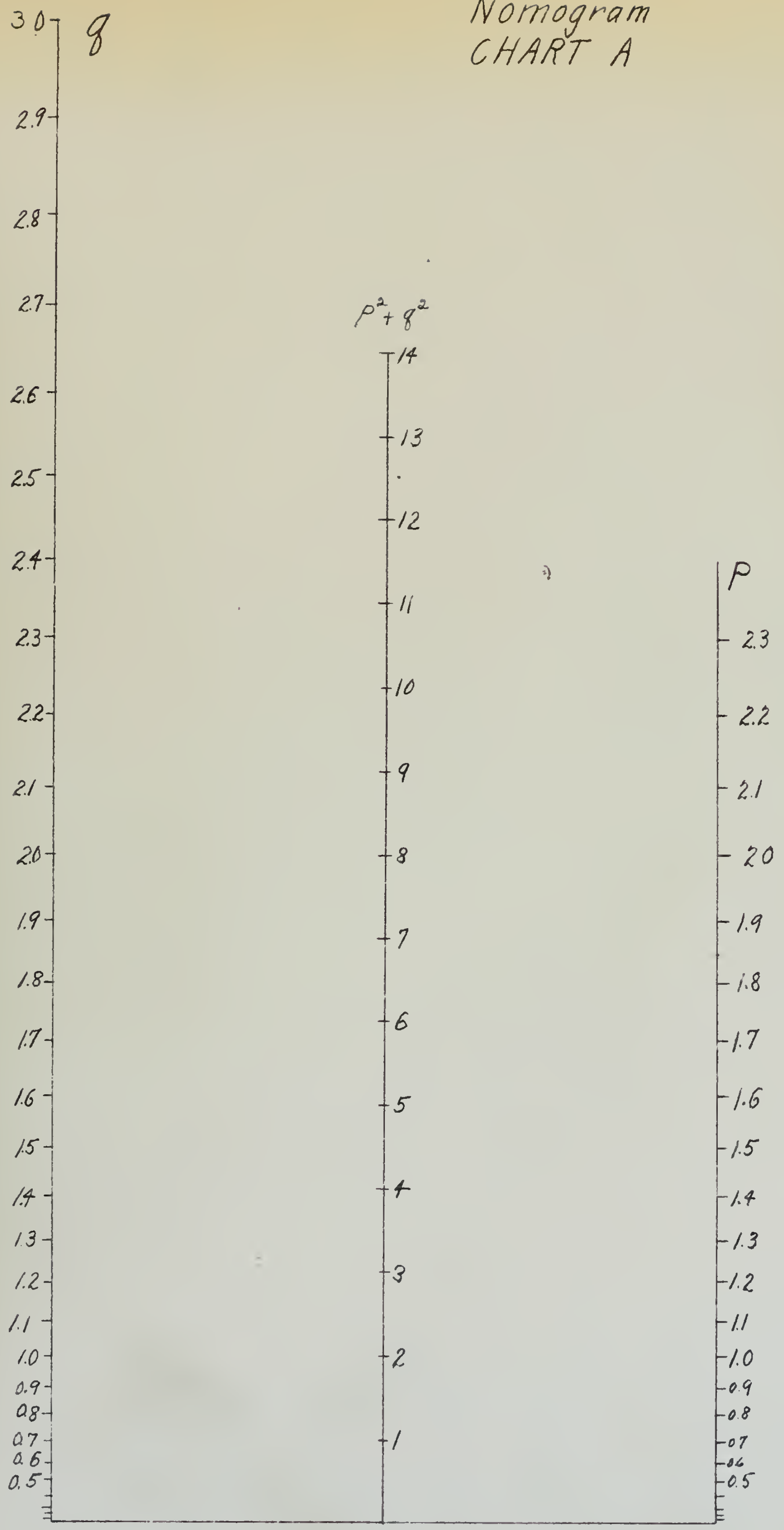

CHART B Fig 7

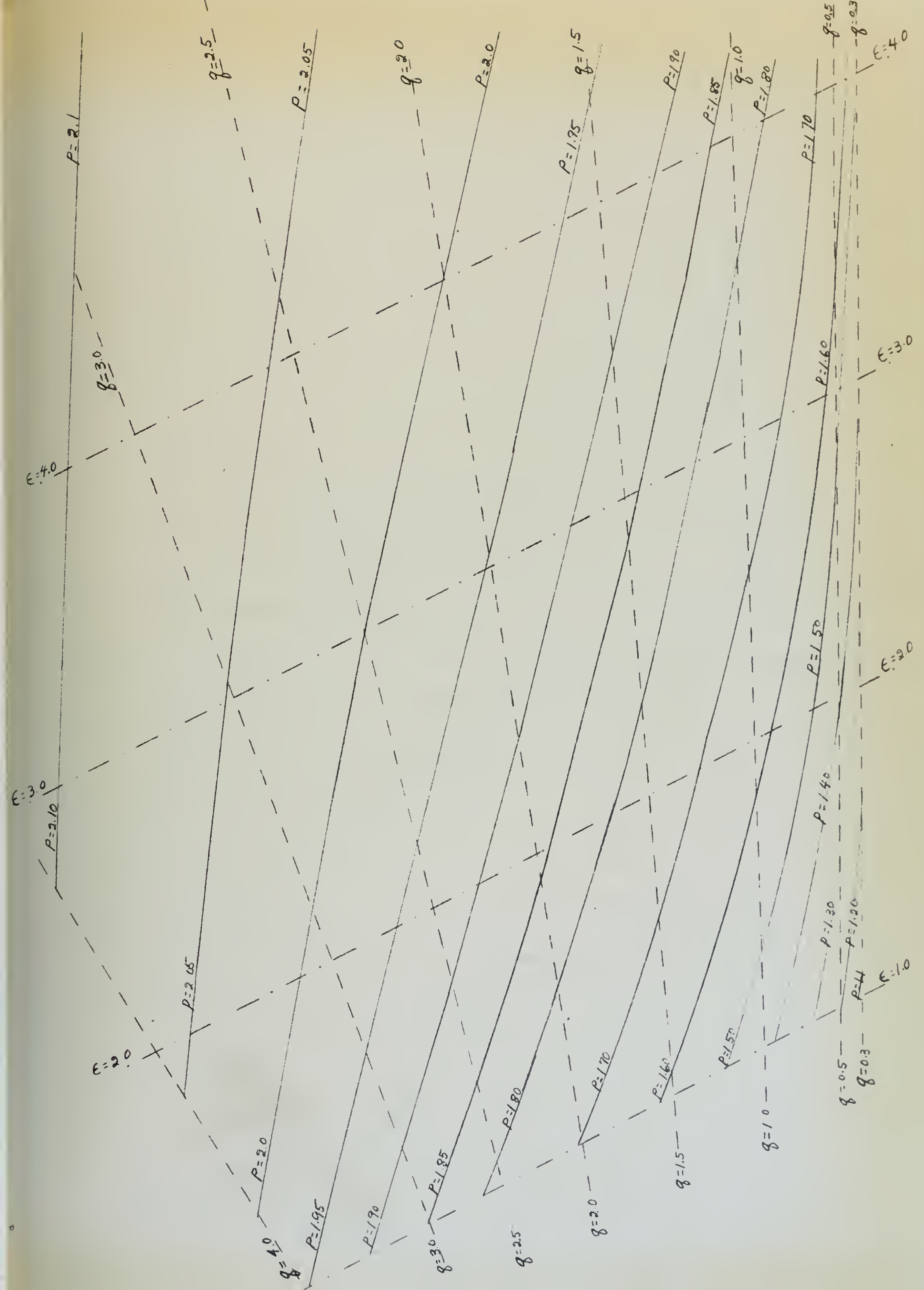

p=2.1
p=2.05
p=2.0
p=1.95
p=1.90
p=1.85
p=1.80
p=1.70
p=1.60
p=1.50
p=1.40
p=1.30
p=1.20
p=2.10
q=3.0
q=2.5
q=2.0
q=1.5
q=1.0
q=0.5
q=0.3
q=4.0
E=4.0
E=3.0
E=2.0
E=1.0

and locate this point on the center column of Chart A. A straight edge pivoted at this point will give the values of p and q allowed for the given dielectric and diameter. Assume a value for q and place the straight edge at this point on the left column, keeping it also at the pivot point of the center column. The corresponding value of p is read where the straight edge intersects the right column.

Now look at Chart B, and mark off or visualize an $\epsilon$ line, corresponding to the given value, running straight and parallel to the dash dot lines. Find the assumed value for q along this line, as indicated by the dashed q lines. At this point, thus located, read the corresponding value of p by eye interpolation between the solid p lines. Compare the values of p as given by Chart B with that obtained from Chart A. If the value of p as given by Chart B exceeds that given by Chart A, then the assumed value of q was too large. Assume a lower value of q and again find the corresponding p values from Charts A and B as before. When the two charts give identical p's for the same q, the solution is correct.

The above is a trial and error method, but it is easily performed and converges very quickly to a solution which is sufficiently accurate for many purposes. It may happen that a solution may be required that does not fall on the chart. It was impossible to make a chart which was readable and of reasonable size without considerable restriction on the range. However, the range selected for the accompanying charts is believed to be useable for most of the practical problems anticipated at this time. If the required solution does not fall on the charts, numerical methods should be used. In order to facilitate these, the values of f and g as functions of p and q, respectively, may be obtained from the plots of these functions, given in Figures 8 and 9. These plots may also be useful to refine the graphic solutions obtained from the Charts A and B, if additional accuracy is desired.

Having solved the equations for the waves in a circular dielectric rod in air, we can now readily calculate the optimum length for a given dielectric constant, diameter , and frequency (equation 192). The next problem is to determine

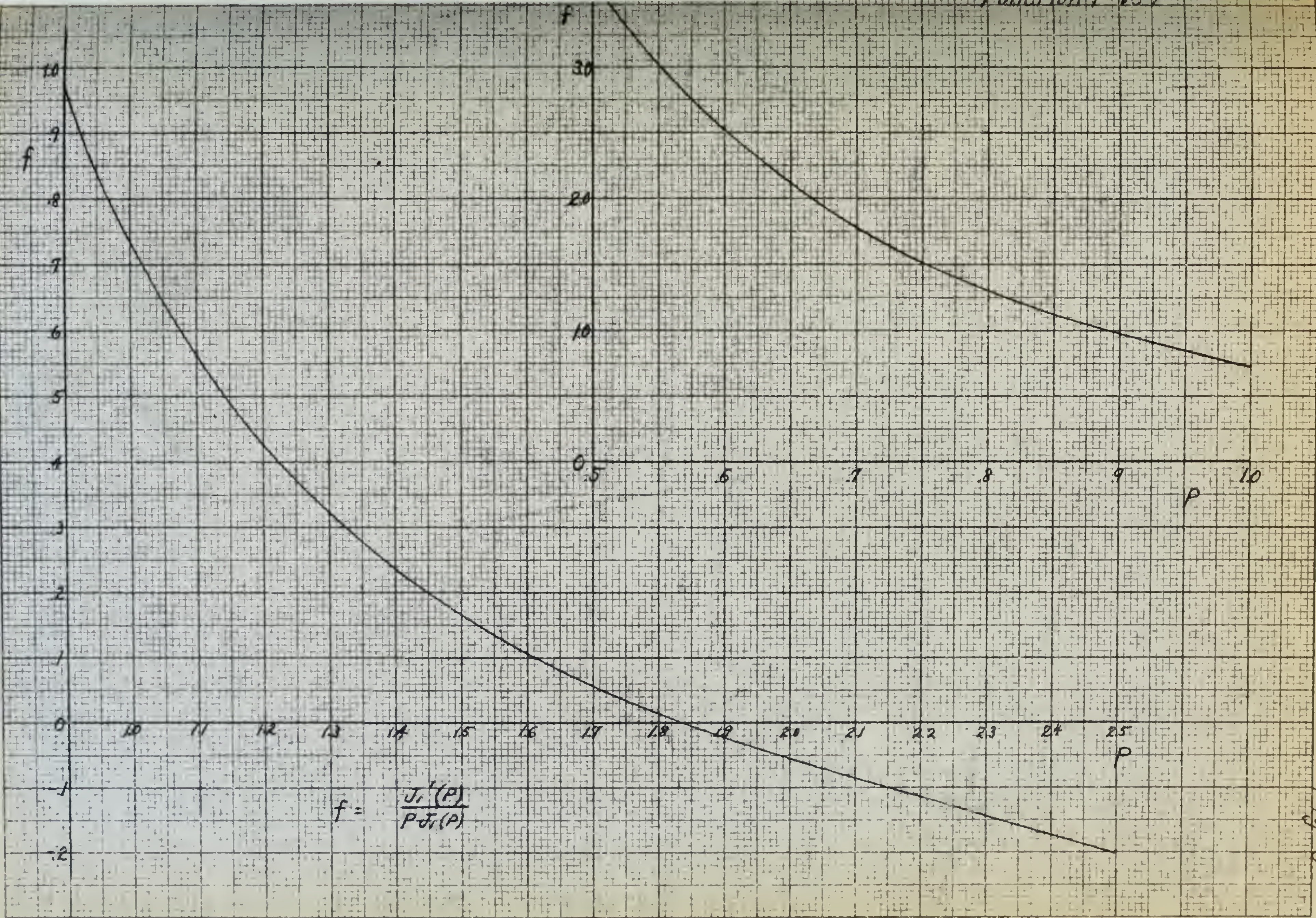


Fig 8

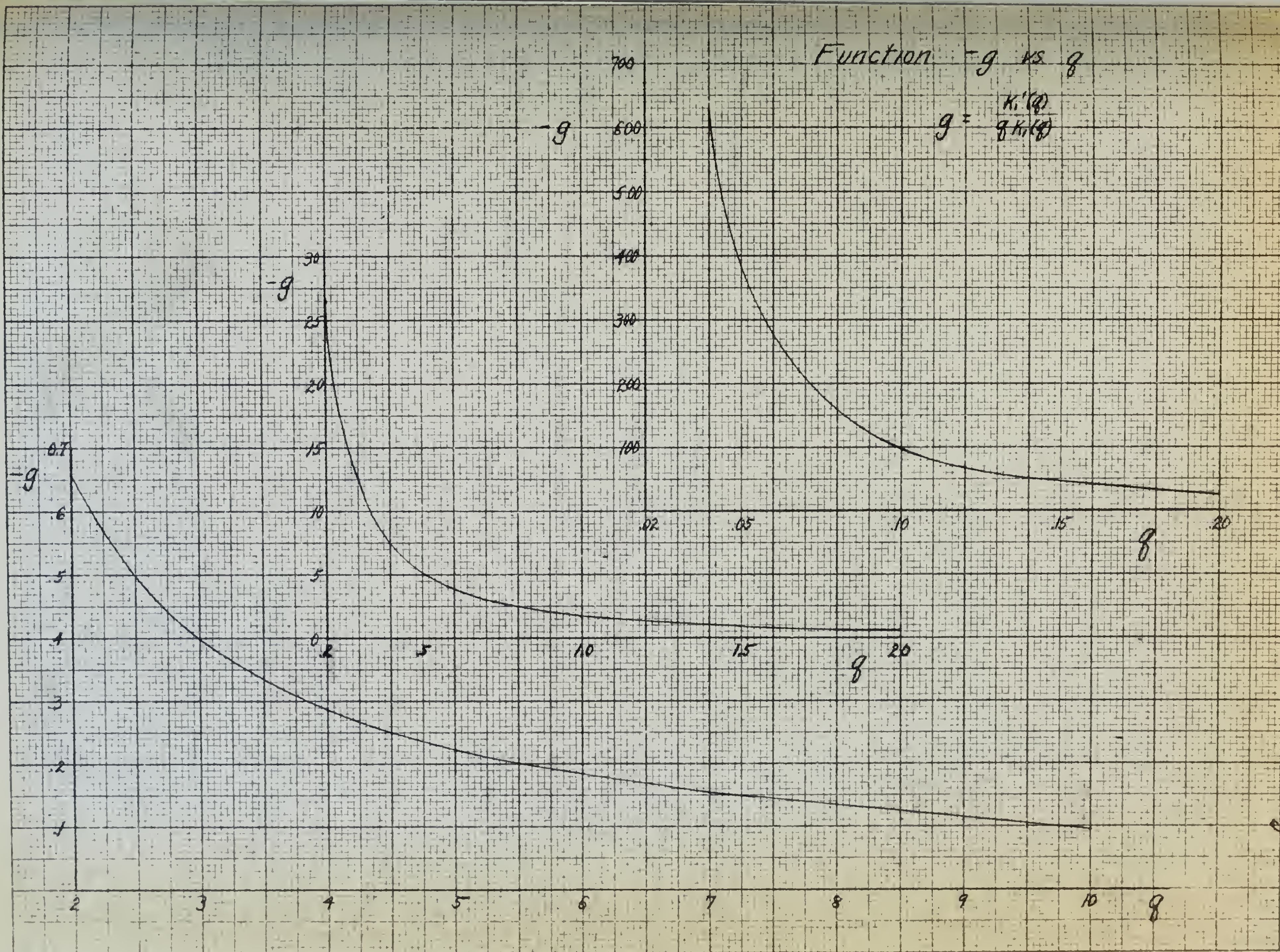


Fig 9

what gain can be expected from the antenna. There is no accepted method for calculating the gain, although several theories have been proposed[11,15]. It is for this reason that we turn to experiment to obtain the gain to be expected for the given conditions. The next chapter will describe the equipment and procedure used to obtain the needed experimental data. After describing these measurements, the data will be discussed and an attempt made to correlate the results with Marsten's theory[11].

It will be noted that the preceding theory has dealt exclusively with the circular cross section rod antennas. The case of the rectangular cross section is much more difficult due to the fact that there are discontinuities on the edges, which are cumbersome if not impossible to account for. Furthermore, there is no convenient coordinate system in which to set down the mathematical expressions. No published theory of electromagnetic waves in dielectric rods of rectangular cross section is available, and consequently for the design of dielectric antennas of these shapes, the experimental data must necessarily be used. It will later be evident that the performance of rectangular rods is very

de

definitely different from that of circular rods.

# CHAPTER 3.

## DESCRIPTION OF EQUIPMENT, PROCEDURE, AND EXPERIMENTAL DATA

The objective of the experimental work was to determine the gain on axis for dielectric antennas excited in the dominant mode, using optimum length rods in each case. These were measured for cylindrical rods of varying cross section diameters, and for rectangular rods with varying sizes in the E dimension, holding the H dimension constant at the width of the standard 3 centimeter wave guide (0.9 inches). A wavelength ($\lambda_0$) of 3.2 centimeters, equivalent to a frequency of $9.37 \times 10^9$ cycles per second, was used for the reason that the components were of convenient size and the equipment for use at this frequency was available. The equipment is shown in Figures 10-14. Two dielectric materials were used for each antenna: Polystyrene ( $\epsilon = 2.56$ ) and Teflon ( $\epsilon = 2.10$ ).

A standard Klystron oscillator was used for a transmitter, but square wave modulation was imposed on the carrier frequency to facilitate detection in the receiver. The transmitter operated from a

Fig. 10

PHOTO NUMBER DATE PRINTED

965-1

Fig. 11

Fig. 12

PHOTO NUMBER DATE PRINTED

9653

Fig. 13


APL
012939
MODULATION
AMPLITUDE
FREQUENCY
E.REPELLER
S.W.R. GAIN
OFF

Fig. 14

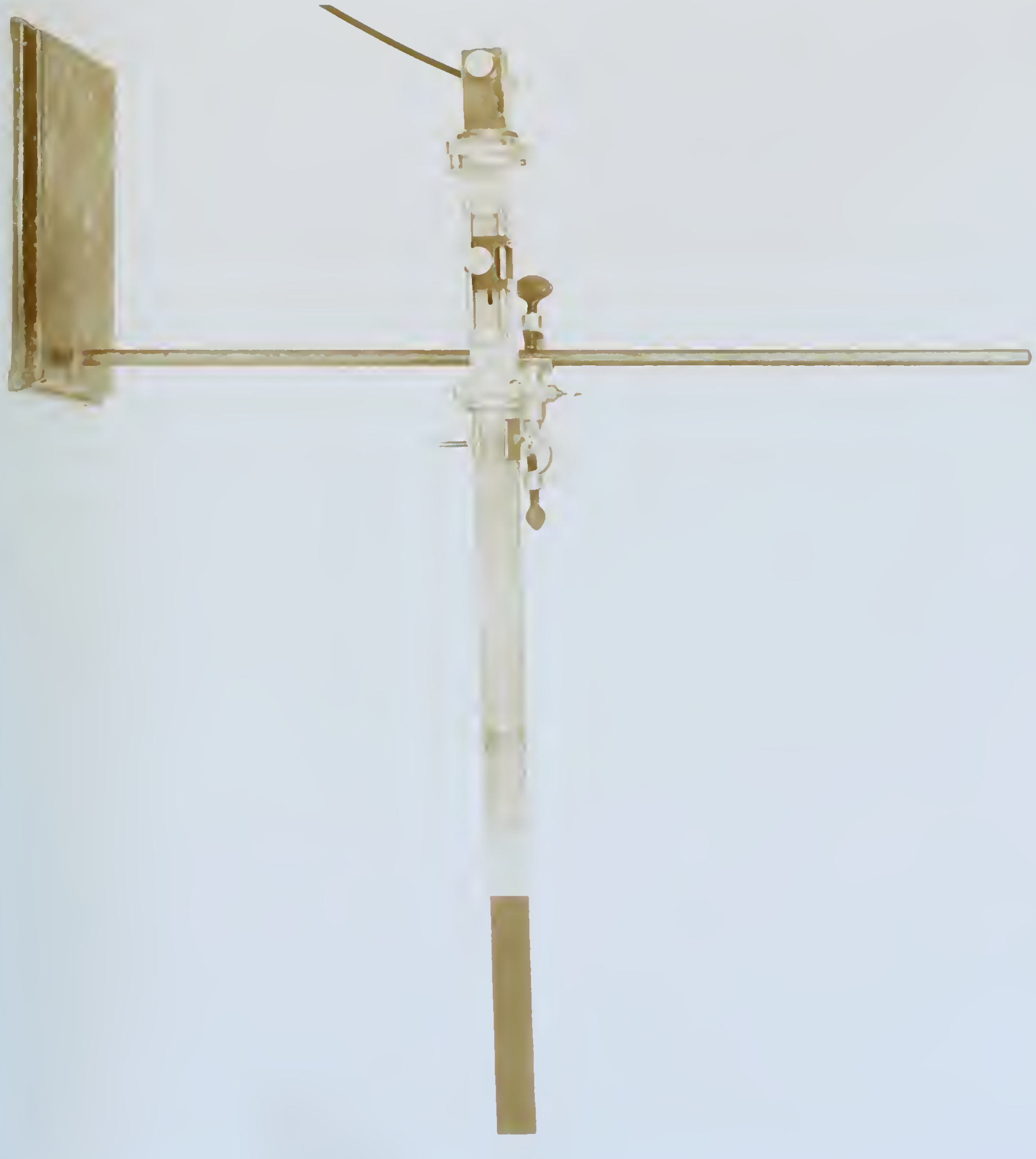

regulated power supply which was fed from the 60 cycle 115 volt power lines through a voltage regulating transformer. The receiver consisted of a crystal detector, amplifier, and voltmeter. As a check on receiver operation, all measurements were repeated using a Pickard and Burns Bolometer Amplifier, model 100. Results were in substantial agreement with those reported and will not be repeated.

The various sizes of dielectrics were fitted into sections of wave guide, made especially for the purpose, tapered down to standard size and fitted with a standard choke. See photographs. The part of the dielectric which fits into the guide was tapered in each case, in order to minimize reflections and reduce standing waves. The elimination or correction for the standing waves proved to be the most difficult problem to overcome. The taper reduced the voltage standing wave ratio (VSWR) in most cases to below 2.0. In every case this was carefully measured and a correction applied to obtain the actual transmitted power, using the well known formula (193)

$$\frac{P_t}{P_i} = \frac{4r}{(r+1)^2}$$

where $P_t$ is the transmitted power

$P_i$ is the incident power

r is the voltage standing wave ratio (VSWR)

Several methods were used to make the measurements. To begin with, the dielectric was used as the transmitting antenna, since receiver power was inadequate to accurately measure the VSWR. The VSWR was measured at the transmitter using a standard standing wave indicator. Later it was found more precise to use a calibrated attenuator together with a slotted section, crystal detector, amplifier, and voltmeter, attenuating as necessary to equate the voltage from the high voltage point to the low voltage point. The method by which the final measurements were made used this equipment, employing an attenuator which had been accurately calibrated by the National Bureau of Standards.

As a further check on the accuracy of the measured gains, the various dielectric antennas were each put at the receiver with a special matching section, and the measurements repeated. For each reading, the matching section was adjusted to maximize readings by the reduction of the standing waves.

Results for the dielectric antennas up to one wavelength in diameter or in the E dimension were in agreement with those measured by the previous two methods. Gains measured for larger antennas were somewhat less, which can be accounted for by the fact that standing waves still existed to an appreciable amount despite the matching section.

Some slight difficulty was encountered with reflections within the room. These were reduced as much as possible by the strategic use of an absorbing screen. As a check on errors which might be introduced due to reflections, the distance from the transmitter to receiver, normally of the order of one hundred wavelengths, was changed in quarter wavelength increments, noting power detected at each range. If appreciable reflections were interfering, there should be alternate addition and cancellation of power observed. It was found that detected power was not appreciably different for these positions a quarter wavelength apart, and it was concluded that any errors from reflections were of little significance.

Before measuring the gains it was necessary first to find the optimum length of the dielectric.

This was done experimentally by observing relative power transmitted, first with the dielectric almost flush with the mouth of the guide, and then out $\frac{1}{4}$ inch and so on with longer lengths using increments of about $\frac{1}{5}\lambda_o$. Near the peak of the transmission smaller increments were used to obtain the exact optimum length. Having the relative power transmitted at optimum length, the test antenna was then immediately replaced by a precalibrated standard horn and the powers compared. This enabled calculation of the relative gain of the test antenna with respect to the standard horn.

The gain of the standard was carefully measured in order to be able to determine the absolute gain; that is, the ratio of the peak intensity of the given antenna to the intensity of an isotropic radiator when both are radiating the same total power. In terms of the effective area, $A_e$, the gain, G, has been shown[22,23] to be

$$G = \frac{4\pi A_e}{\lambda_o^2} \tag{194}$$

The effective area is the ratio of the power received at the antenna to the power per unit area in the incident wave.

The absolute gain of the standard horn was measured by several of the methods which have been developed and published[5,12,20]. One of these[20] will be briefly described here, which makes use of two identical antennas. The standard horn was attached to the transmitter and an identical one used on the receiver. Under these conditions it is easily shown[20] that

$$(195) \qquad \frac{P_R}{P_T} = \left(\frac{G\lambda_0}{4\pi d}\right)^2$$

where $P_R$ is the received power, $P_T$ is the transmitted power, and d is the distance between the transmitting and receiving antennas. To determine the ratio of received power to total transmitted power, the transmitter and receiver were coupled directly together, except for a calibrated attenuator between. With a large but accurately measured amount of attenuation inserted, a particular receiver voltage was noted. Then the two antennas were attached respectively to the transmitter and receiver and separated by an accurately measured distance (several feet), and the attenuation of the transmitter reduced until the same receiver voltage was obtained.

The difference in the amount of attenuation in the two cases gave the ratio of $P_R$ to $P_T$ in decibels, from which G could easily be calculated.

Presentation of Data

Three alternatives in the presentation of experimental data have been considered, and these will be briefly mentioned to show the reasons for the selection of the one given.

(a) Report the relative gain of the dielectric antenna compared to the gain of the feeding wave guide with the dielectric removed. This would permit a direct comparison of the power on axis with and without the dielectric which would show clearly the effect of the dielectric in directing the beam. However this method was excluded, because the experimental data would not be reproducible unless the feed structures were identical. Gain of open mouth feeds are not precisely predictable and there would be no way to obtain absolute gain or effective area from these data.

(b) Report the absolute gain of the dielectric antenna; that is the power on axis relative to an

isotropic oscillator emitting the same total power. This is better, but here again variations in the metallic feed structures would cause variation in the absolute gain. Furthermore, as shown by equation (194) above, the scales would have an artificial multiplier of $4\pi$.

(c) Report the effective cross section area relative to the physical cross section area. This is the method chosen because: (1) this presentation eliminates the undesired effect of variation in feed structures; (2) as cross section areas are allowed to grow, the effective cross section areas also grow, and these tend to become equal. In other words, the captured energy tends toward that physically intercepted by this area. Therefore, a plot of effective area versus physical area will verge toward a straight line with unit slope passing through the origin regardless of the dielectric used; and (3) an extremely useful piece of information concerning any antenna is its effective cross section area. From this figure it is a simple and direct calculation to obtain the total energy gathered by the antenna in a field of a given strength.

This third method of presentation, in addition to providing the engineer the very useful information

of maximum capture area for various dielectrics of various sizes, illustrates the variation of capture area from the actual area in the sizes of the order of a wavelength, and shows how these should converge to the 45° line as dimensions increase toward optical sizes.

## Choice of Scales

Consideration was given to reporting dimensions directly in centimeters or inches. This would enable an engineer, employing wavelengths the same as used here (3.2 cm) to use the data directly. However, this was rejected because the value of these data is not limited to any particular wavelength. Dimensions are therefore given in non dimensional form; that is, lengths in wavelengths and cross section areas in square wavelengths. Although this requires conversion of practical units to this system to enable usage of the data, it has the advantage that the data are applicable to a very wide band of wavelengths.

A plot of effective area versus actual cross

section area for the cylindrical dielectric antennas measured is given in Figure 15. Figure 16 is the same plot for rectangular cross section antennas. Figures 17 and 18 are also enclosed for completeness giving the absolute gains of cylinders and rectangular cross sections, respectively, versus cross section area.

It will be noted that measurements were not obtained for cylinders of large enough diameter to show convergence of the effective area toward the actual area. In the larger diameter circular cylinders, the mode tended to shift to the $m = 0$ mode which gives a null on axis. No way to prevent this was devised. There was also a practical limit to the measurements on the low side, with the time and facilities available. For small cross section rods the optimum length becomes unmanageably long, and the thin rods tend to sag. Furthermore, these thin long rods require a long range in order to put the field meter in the far zone.

The present technique does not permit extension of the range of measurement for circular rods, and the possibility of existence of TM modes in these dielectrics is a disturbing factor. The

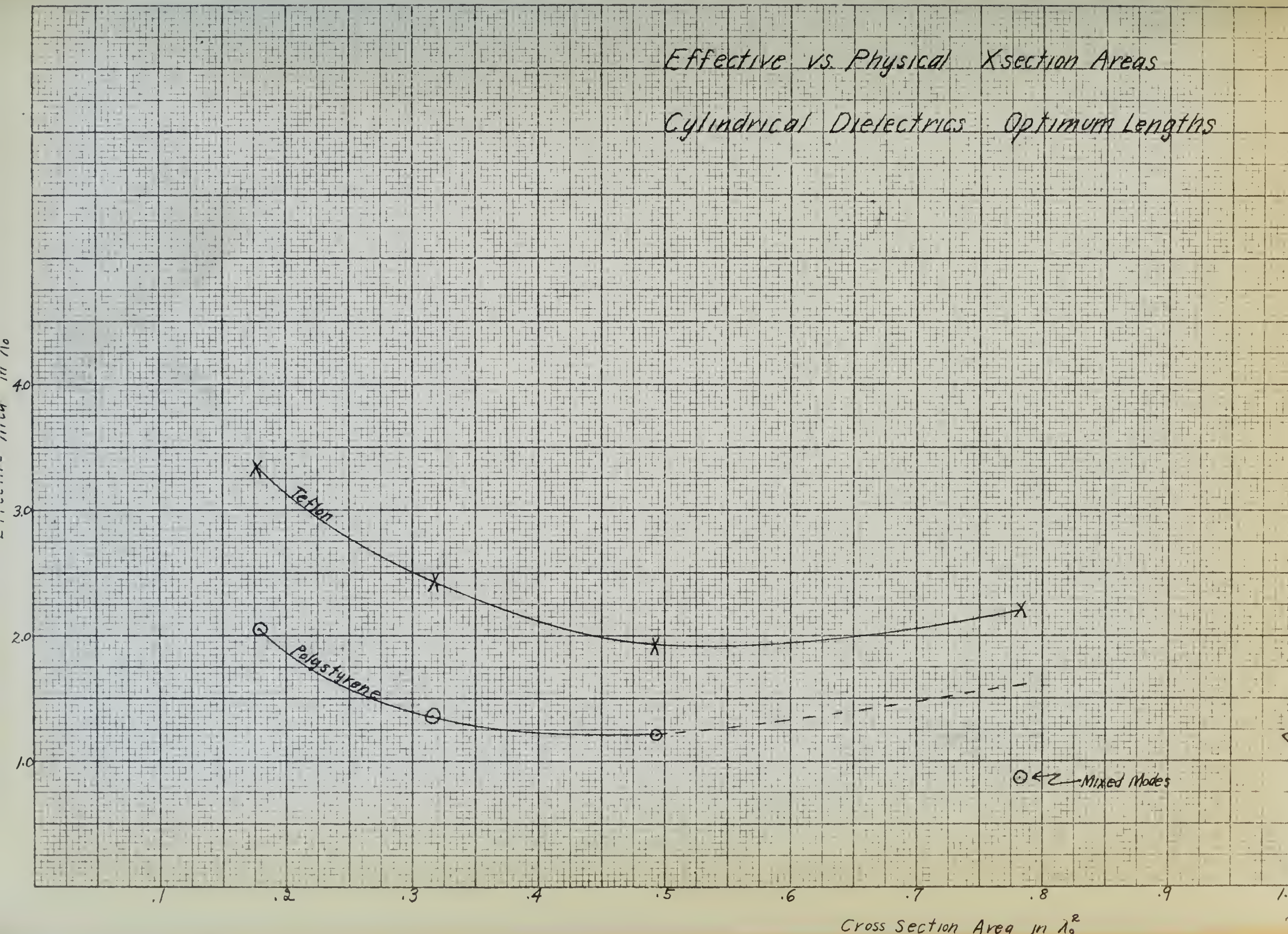

Effective vs. Physical Xsection Areas
Cylindrical Dielectrics Optimum Lengths
Teflon
Polystyrene
Mixed Modes
4.0
3.0
2.0
1.0
.1
.2
.3
.4
.5
.6
.7
.8
.9
1.0
Cross Section Area in $\lambda_0^2$


Fig 15

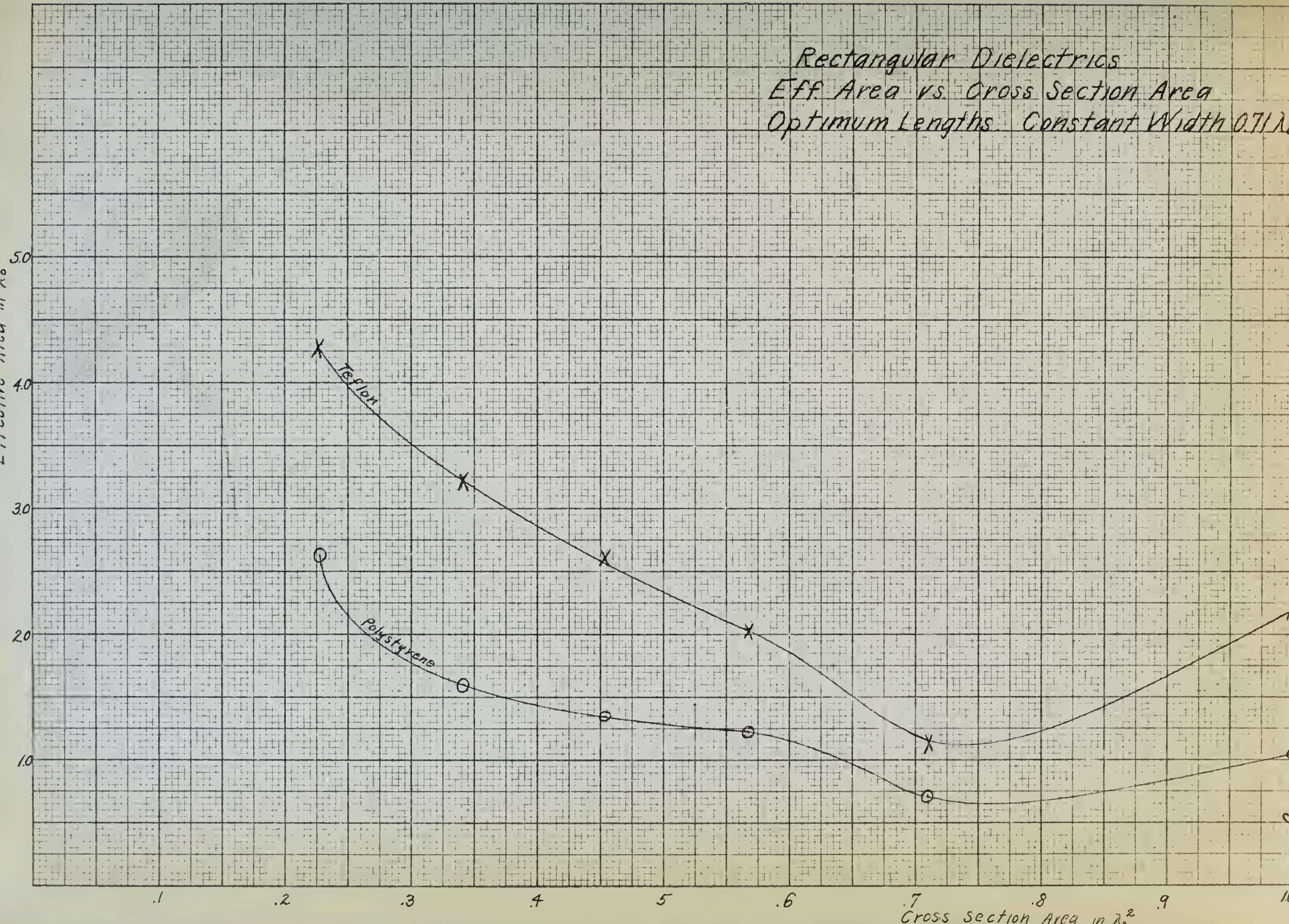

Rectangular Dielectrics
Eff. Area vs. Cross Section Area
Optimum Lengths Constant Width 0.71 λ₀
Teflon
Polystyrene
5.0
4.0
3.0
2.0
1.0
.1
.2
.3
.4
.5
.6
.7
.8
.9
1.0
Cross Section Area in λ₀²

Fig 16

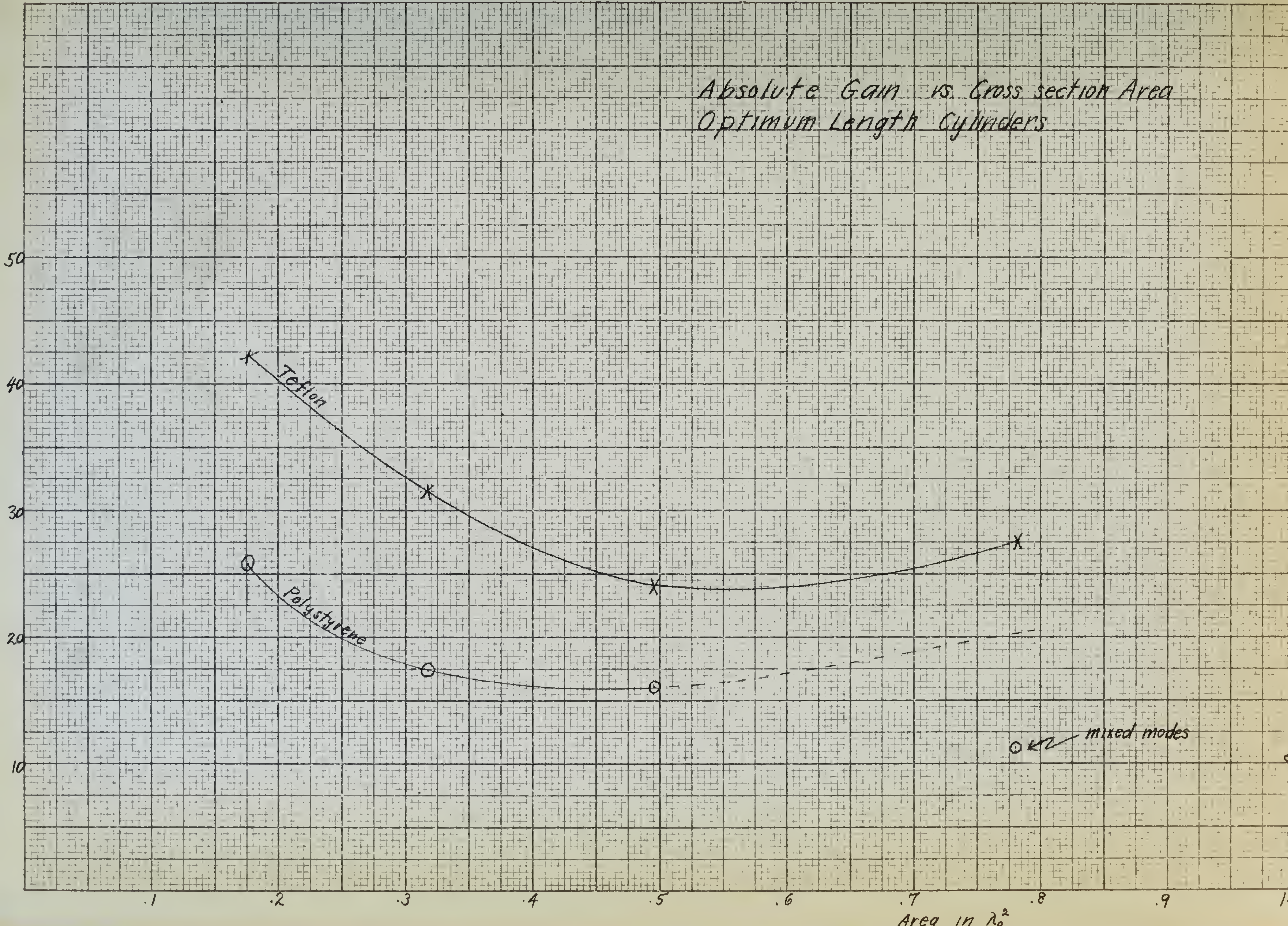

Absolute Gain vs. Cross section Area
Optimum Length Cylinders
Teflon
Polystyrene
mixed modes
50
40
30
20
10
.1
.2
.3
.4
.5
.6
.7
.8
.9
1.0
Area in $\lambda_o^2$


Fig 17

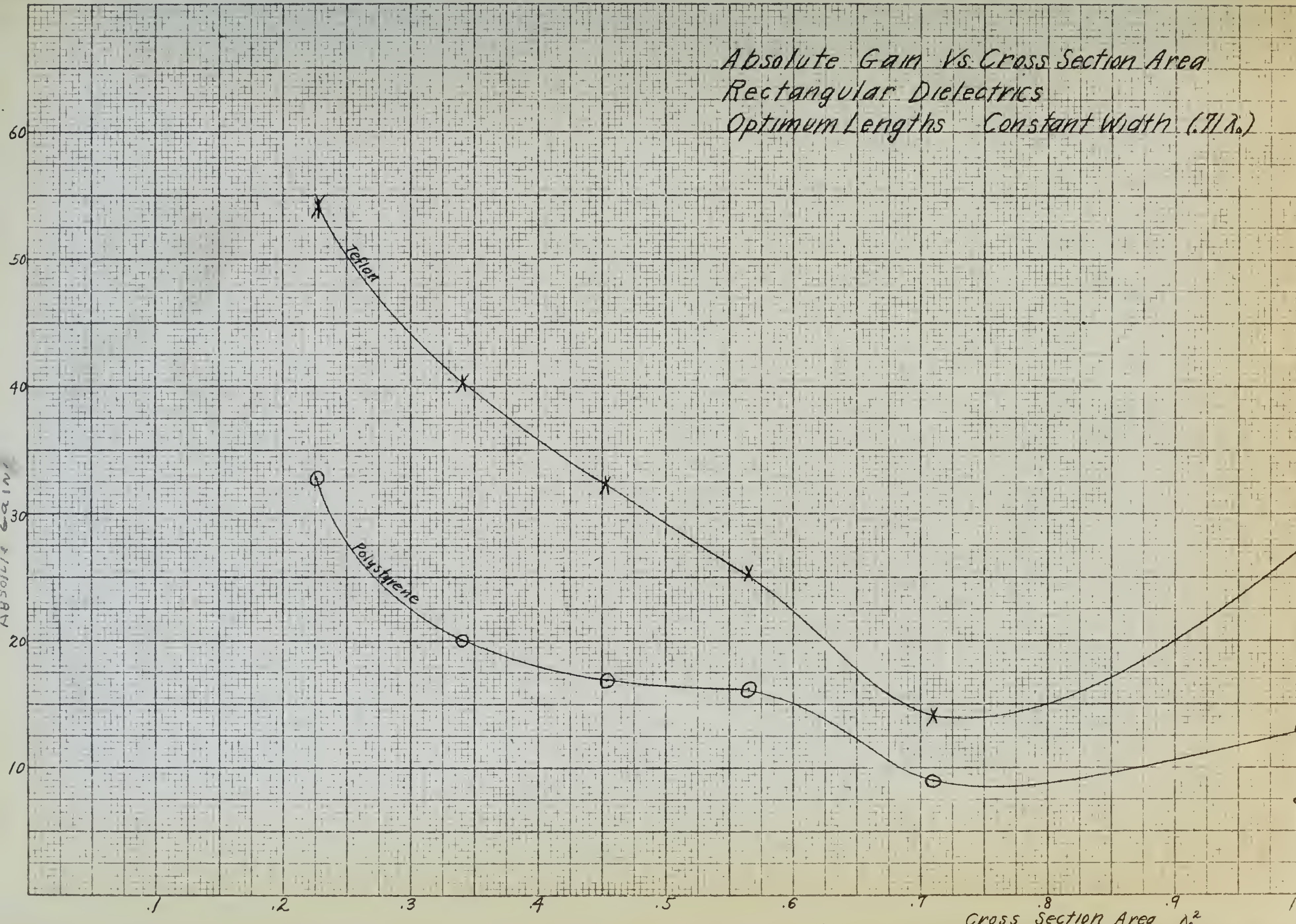

Absolute Gain Vs. Cross Section Area
Rectangular Dielectrics
Optimum Lengths Constant Width (.71 λ₀)
Teflon
Polystyrene
60
50
40
30
20
10
.1
.2
.3
.4
.5
.6
.7
.8
.9
1.0
Cross Section Area λ₀²


Fig 18

apparent irregularity of the polystyrene rods may be caused by this phenomenon. In order to reduce the probability of spurious modes in the exciting radiator for the larger areas, conical horns were also tested with polystyrene cylinders, with the following results

| Horn diameter | Horn Physical Area | Antenna Capture Area |
|---|---|---|
| $2\frac{1}{4}$" | 2.5 $\lambda_0^2$ | 3.78 $\lambda_0^2$ |
| $3\frac{1}{4}$" | 5.25 $\lambda_0^2$ | 5.24 $\lambda_0^2$ |

Here the trend of antenna effective area toward actual area is noted. The horns were far from optimum from the point of view of radiation pattern, however, and the lens antennas were also probably not optimum. Therefore, convergence of optimum cylinders toward the expected asymptote would not be closely realized until the experiment reached much larger areas than the above figures indicate.

In the rectangular rods, no tendency of the mode to shift was observed, but other practical difficulties prevented extension of the range of sizes. In order to prevent cut off in the antenna feed, when using small sizes, the H dimension was

set at a constant value of .71 $\lambda_0$. Small areas, then, would have required very long and thin sections which would have caused the same difficulties mentioned above for circular rods. The larger cross section areas, where the E dimension was large compared to the constant H dimension, gave radiation patterns which were relatively narrow in the plane parallel to the E dimension, and relatively broad in the plane parallel to the H dimension, thus giving reduced gain on axis. It was found that if the cross section area had been made more nearly square, a radiation pattern more nearly circular would have been produced, and thereby increasing gain on axis. The gain on axis, being a function of the radiation pattern, then, is dependent on the shape of the cross section. For small cross sections this effect is small, but for cross sections of a wavelength or larger the effect is very pronounced. A way to avoid this would be to properly shape the front surface of the dielectric, or to taper the rod. Neither of these were attempted here. The end surfaces of all the antennas tested were plane.

It was evident that the larger rectangular

dielectrics would give higher powers on axis if the cross section was approximately square. Therefore, as the wavelength region is approached in Figure 16, the larger physical cross section antennas appear at a disadvantage. Perhaps a better comparison in this region would have been to compare the antenna capture area to the capture area measured for the same metallic feed with the dielectric flush with the metallic aperture (zero length antenna). This method of reporting would have brought the larger areas more in accord with the following table, measured only for polystyrene.

| Feed Horn Dimensions | Physical Area in $\lambda_0^2$ | Capture Area of Feed Horn | Capture Area of Antenna |
|---|---|---|---|
| .9 x 1.8" | 1.02 | 0.64 | 1.03 |
| $1\frac{1}{2}$ x $1\frac{1}{2}$" | 1.42 | 1.0 | 1.7 |
| $2\frac{3}{4}$ x $2\frac{3}{4}$" | 4.76 | 4.75 | 5.3 |

This table shows the trend, predicted previously, of the capture area of the optimum length antenna to approach the physical cross

section as the latter becomes many wavelengths in each direction. The shaping of these larger antennas was only attempted approximately and somewhat larger capture areas would be expected if optimum shapes had been employed.

# CHAPTER 4.

## DISCUSSION OF RESULTS AND ATTEMPTED CORRELATION WITH EXISTING THEORIES

The curves of effective area versus cross section area, Figures 15 and 16 of Chapter 3, show that considerable increases in effective areas over actual areas are obtainable if the physical areas are small (less than a square wavelength). These effective areas are quite high for small physical areas and reduce toward the physical areas as sizes become larger. The trend is apparent for the rectangular dielectrics, but could not be demonstrated with circular cross section because of shifting of the mode within the dielectric despite excitation by the $n = 1$ mode.

As previously pointed out, the design of the dielectric antenna above a wavelength in cross section area is still not understood. The gain on axis, on which the experimental results are based, is a function of the shape of the total pattern.

The gain is measured by sampling this pattern on the prolonged axis of the dielectric. This spread in pattern is particularly apparent in these data in the sizes immediately above a square wavelength. In this region ray optics play an important role; and yet customary treatments by ray optics fail because of the considerable phase gradients due to the adjacent metallic structures supporting the radiator. In fact, such a treatment would involve serious difficulties. In the present project, the problem would be further complicated by the absence of an accurate means to determine the complete wave characteristics of each of the various feed horns used. Proper lens shaping would necessarily have to be based on a knowledge of the phase front of the horn to be lensed. However, to show the trend beyond the one wavelength region toward the expected $45^{\circ}$ asymptote a few measurements were attempted in which the face of the dielectric was shaped by means of trying many combinations of various size blocks so as to obtain a stepped profile. The best gains were found in these larger shapes when the profiles resembled optical lenses in physical shape, and the larger the area the more nearly the

true optical shape is required to optimize gain. This is in contrast to smaller cross section areas, where shaping of the front face had little effect, and experimental measurements were very consistent. Evidently the phase gradients within the smaller dielectrics play a much less significant role.

Because of the fact that these data are based on unoptimized profiles, it is apparent that gains of optimized shapes would be higher than here reported, and convergence to the $45^{\circ}$ asymptote would occur much further out. It is expected that when better theories are available for the design of lenses in the wavelength region, curves similar to those of Figure 16 could be expected to converge monotonically to a line of unit slope, and to reach the asymptote only after dimensions are such that the areas are many square wavelengths.

One experiment was attempted some years ago to "lens" a 30 inch parabolic aperture on X band, and it was not found possible to detect any increase in effective area. As the aperture grows, optical lenses are obtained, where effective area is strictly proportional to actual area. In a recent report[25] of experiments sponsored by the U.S. Army Signal Corps, tests were revealed on a spherical Lucite lens of cross section area 985 square wavelengths. Gains

reported, after correction for the losses occurring in Lucite, indicate an effective area of 635 square wavelengths. The apparent discrepancy is due to the fairly narrow illumination used in this experiment. The illumination duplicated the usual radar dish illuminations and resulted in the expected aperture utilization factor of 65% commonly employed in radar dish antennas. This shows that effective areas actually do converge to the physical areas utilized in large sizes.

Converging lenses have been made for the wavelengths considered herein. While these appear to give a tremendous power at their designed focal point, a more thorough discussion would show that they merely operate as converging devices, obeying to a first approximation the half power law

$$\frac{d}{\lambda_0} = \tfrac{1}{2} \text{ power angle of radiation}$$

They do not increase the effective area of the aperture.

## Marsten's Theory

A very excellent theoretical treatment of the

dielectric antenna of circular cross section is given by Marsten in a recent report[11] published by the U.S. Naval Research Laboratory. A circular dielectric rod is excited in any single mode, and the equations used for the waves are equivalent to those given in Chapters 1 and 2. From these are calculated equivalent electric and magnetic current distributions over the surfaces, in accordance with Schelkunoff's Equivalence Theorems[18]. Then the radiation field is computed using the method of Schelkunoff, first for the field arising from the equivalent sources at the sides of the rod, $E^{(1)}$ and then for the equivalent sources at the end of the rod, $E^{(2)}$ . Certain factors common to both expressions are dropped, since only the relative field is of interest, and the final expressions for the θ components are given as follows

$$E_\theta^{(1)} = -\cos m\phi \; \ell \; \frac{\sin\chi}{\chi} J_m(P) \Big[ (\eta\, \delta \cos\theta + 1) J_{m-1}(L) - \frac{2\eta B \sin\theta}{A} J_m(L) + (\eta\, \delta\cos\theta - 1) J_{m+1}(L) \Big] \tag{196}$$

(196) continued

$$E_\theta^{(2)} = -\cos n\phi \, \frac{2a^2}{p^2} \, j e^{jx} \left[ \cdot \frac{n}{L} \left( \eta h \delta \cos\theta + \omega \mu_1 \delta \right) J_n(L) J_n(p) + \frac{(\eta \omega \varepsilon_1 \cos\theta + h) p}{L^2 - p^2} \left\{ L J_n(L) J_n'(p) - p J_n(p) J_n'(L) \right\} \right]$$

The expressions for the other components of the field will not be repeated, since only the power on axis is of interest here.

The notation is the same as given herein, except as follows:

$j = i = \sqrt{-1}$

$\beta = \omega \sqrt{\mu_0 \varepsilon_0} = \frac{2\pi}{\lambda_0}$

$\ell$ - - - - - - - - length of rod. Since optimum length $(\ell_0)$ is here considered, substitute $\frac{\lambda_0}{2(n_a - 1)}$

$\chi = \pi \left( \frac{\ell}{\lambda_0} \cos\theta - \frac{\ell}{\lambda_1} \right)$

On axis $\cos\theta = 1$ and for optimum length $\chi = -\frac{\pi}{2}$

$L = \beta a \sin\theta$ On axis $L = 0$

A and B are functions which are always finite and non-zero

$$\delta = \frac{-\frac{\omega\epsilon_1}{p} J_n'(p) K_n(q) - \frac{\omega\epsilon_2}{q} K_n'(q) J_n(p)}{n h \left(\frac{1}{p^2} + \frac{1}{q^2}\right) J_n(p) K_n(q)}$$

which upon simplification and substitution from equations (187) and (194) becomes in our notation

$$\delta = \frac{1}{\eta} \frac{(\epsilon f + g)^{1/2}}{(f + g)^{1/2}} = + \frac{V}{\eta}$$

By actually substituting numbers, it is found that $\delta$ has a plus value for all dimensions under consideration, and so the positive sign should be used after extracting square root.

Assuming n =1, $\theta = 0$, $l = \frac{\lambda_0}{2(n_a - 1)}$, and $\phi = 0$ the above equations reduce to

(197)
$$E_\theta^{(1)} = -\frac{1}{\pi} \frac{1}{n_a - 1} J_1(p)(V+1)\,\lambda_0$$

(198)
$$E_\theta^{(2)} = -\frac{\pi}{2}\left(\frac{2a}{\lambda_0}\right)^2 \frac{1}{p^2} J_1(p)\left[V(n_a+1) + \epsilon + n_a\right]\lambda_0$$

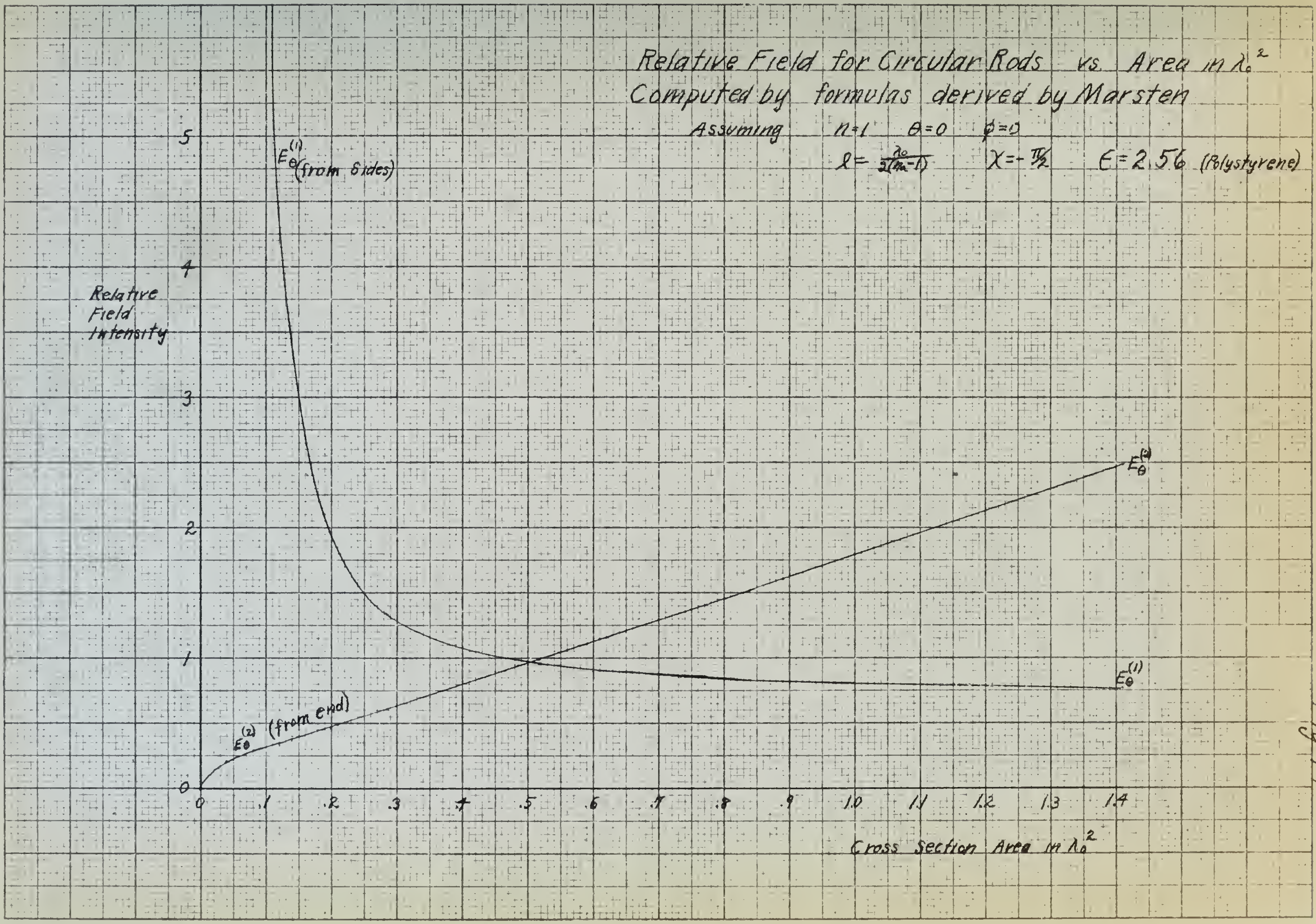
Relative Field for Circular Rods vs. Area in $\lambda_0^2$
Computed by formulas derived by Marsten
Assuming $n=1$ $\theta=0$ $\phi=0$
$l = \frac{\lambda_0}{2(m-1)}$ $\chi = -\pi/2$ $\epsilon = 2.56$ (Polystyrene)
Relative Field Intensity
$E_\theta^{(1)}$ (from Sides)
$E_\theta^{(2)}$ (from end)
$E_\theta^{(2)}$
$E_\theta^{(1)}$
0
1
2
3
4
5
0
.1
.2
.3
.4
.5
.6
.7
.8
.9
1.0
1.1
1.2
1.3
1.4
Cross Section Area in $\lambda_0^2$

Fig 19

A plot of effective area for optimum length computed as above is given in Figure 20, where the abscissa is taken as the physical area.

The gains calculated by Marsten's theory show the same general trend as the experimental data of Chapter 3 show. The principal exceptions are, first, that all are much higher in value than could be found experimentally, and, second, it is noted that the theory does not hold at all when dimensions are small enough so that $n_a$ approaches 1. Equation (202), the expression for the contribution from the sides, has a denominator, $\pi(n_a - 1)$ which approaches zero as $n_a$ approaches 1 with decreasing diameters. The term $J_m(\rho)$ in the numerator also approaches zero as the diameter goes to zero, but this occurs much more slowly. The result is that powers on axis as indicated become extremely high for small rods. These enormous powers do not conform to experimental observations.

The question of identical phases for the radiation from the side walls and from the ends does not appear to be correct from a physical viewpoint. The phase within an optimum length rod emerges one half period later than the wave travelling the same

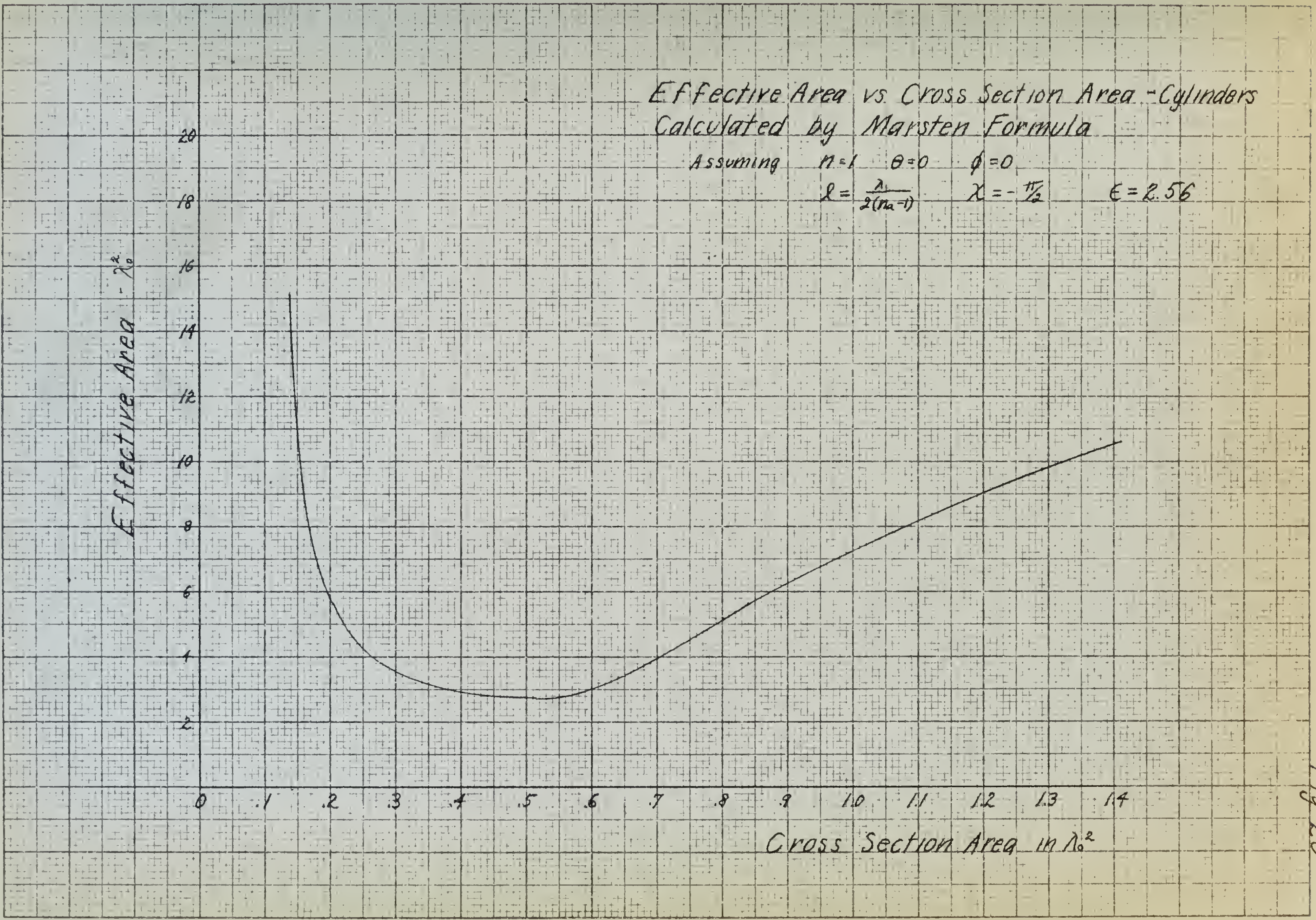
Effective Area vs. Cross Section Area - Cylinders
Calculated by Marsten Formula
Assuming $n=1$ $\theta=0$ $\phi=0$
$l=\frac{\lambda_1}{2(n_a-1)}$ $\chi=-\frac{\pi}{2}$ $\epsilon=2.56$
Effective Area - $\lambda_o^2$
20
18
16
14
12
10
8
6
4
2
0
.1
.2
.3
.4
.5
.6
.7
.8
.9
1.0
1.1
1.2
1.3
1.4
Cross Section Area in $\lambda_o^2$

Fig 20

distance in free space. Along the rod the phase relative to the end must certainly lead by something less than a half period but more than zero. If, in the theory, some adjustment to these phases were made, it is possible that the theory might fit the experimental findings more closely.

Another interesting point is noted from equations (196) and (197). As the diameter becomes very large p approaches zero. ( $p = a\sqrt{k_1^2 - h}$

and at large diameters h approaches $k_1$). If n =1, then $J_n(p) = 0$, and the right sides of both equations vanish. We must conclude from this, if the theory holds for large sizes, that no radiation could occur from an antenna of very large diameter if the optimum length is determined as calculated above.

## Wilkes' Theory

An explanation for the peculiar behavior of gains in the region of areas of a fraction of a square wavelength is given in a theory proposed by Wilkes[24] on the Interaction of Radiant Energy. It has been shown experimentally that the effective

areas in this region are considerably greater than the physical cross section areas, although powers are definitely limited. Presently published theories on dielectric antennas of circular cross section would allow an unlimited growth of capture area with diminishing cross section areas.

Wilkes, however, has shown experimentally that the power growth is in reality not unlimited, but that the capture area for small cross sections is limited. A simplified qualitative outline of his approach is given below to indicate the method by which he arrives at a solution of this hitherto unaccountable phenomenon.

As the propagation down a very thin dielectric rod is a plane wave, the phase and group or photon velocities are assumed by him to be identical. By an ingenious technique, he has been able to measure the phase velocities in extremely short lengths of dielectric and to compute the velocities down to a zero length. In these thin dielectrics the energy starts at its critical velocity, $\frac{c}{\sqrt{\epsilon}}$ for very short lengths and approaches c for increasing lengths. Knowing this rate of change of velocity it is possible to conceive of the photons following

describable ballistic trajectories. This, however, requires the concept of an applied force to photons of finite mass which exhibit properties of inertia. Since the photon mass is at present unknown, except for de Broglie's controversial findings[26], direct use of ballistic principles to calculate this force is not possible. Nevertheless, with this concept in mind, a consideration of the nature of the forces brought to bear on the photon reveal a behavior closely compatible with experimental observations.

Postulating the existence of forces between the internal and external fields, which we have just noted, it follows that there is a transfer of work or energy from one of these fields to the other. The medium of energy exchange is photons of a frequency determined by the excitation.

Wilkes has found experimental evidence of the existence of these forces; in fact his calculations and experiments support the existence of the force as composed of two parts. One part is a pressure action proportional to the difference in velocities of the two fields. The other is a function of the total phase lag and appears

gravitational in nature. The magnitude of this action is found equal to the radiant pressure and parallels in this respect Mandelker's theory[27] of gravitation.

From Quantum Electrodynamics, Wilkes finds that the quanta in the accelerated dielectric fields become negative and present holes. He then allows these holes to be filled in to the limit allowed by the statistical laws of a degenerate gas, and by means of these calculations arrives at the two saturation points shown on Figure 21 as the lowest cross sections reported. These points have been confirmed by his experiments. The other points of Figure 21, namely those for cross sections greater than 0.2 square wavelengths, are a repetition of the data obtained in Chapter 3. Obviously, if the physical area drops to zero, the capture area will also go to zero, and this seemingly trivial statement permits the completion of the curves of Figure 21.

Fig. 21

Capture Areas Rectangular Dielectrics

Constant width of 0.71 $\lambda_0$

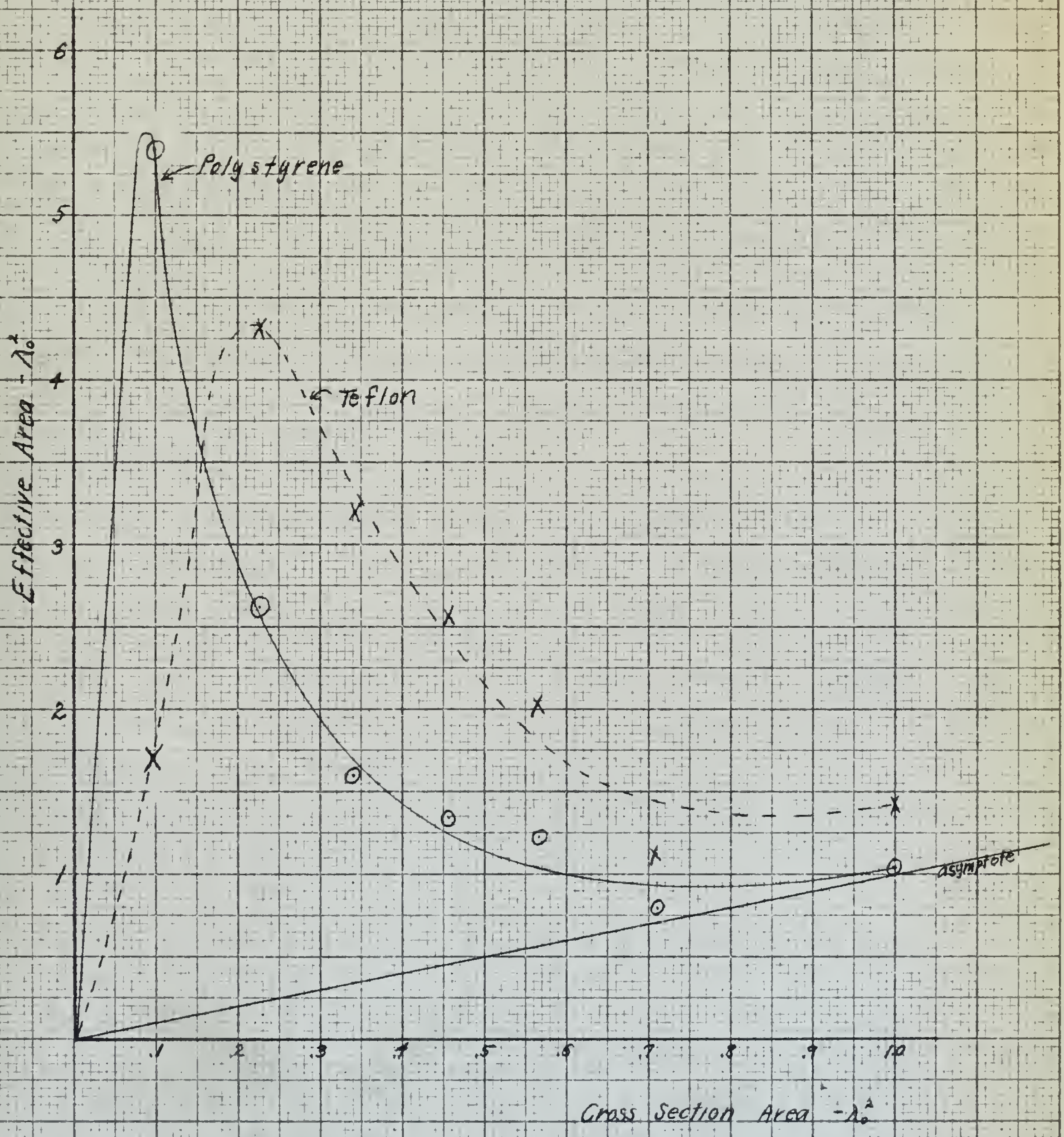

## Conclusion

It is believed that no theory based purely on Maxwell's equations will suffice to explain the peculiar behavior of gains in the very small cross section region. As stated early in this paper, Maxwell's equations hold with certainty only for large scale electromagnetic phenomena, and when dimensions are reduced to fractions of a wavelength, they cannot be relied upon. The true explanation of very small dielectric antennas must come from quantum electrodynamics, as proposed by Wilkes, and the data obtained in Chapter 3 appear to be in close agreement with this theory.

As dimensions grow larger, effective areas of dielectric antennas, if shaped for optimum gain, remain greater than the physical cross sections, but will tend monotonically toward these areas. After areas have reached several square wavelengths, effective area of optimum shaped dielectrics can be closely approximated by the actual physical area.

## GLOSSARY OF SYMBOLS

| | |
|---|---|
| E | Electric Field Intensity vector |
| H | Magnetic Field Intensity vector |
| D | Electric Displacement vector |
| B | Magnetic Induction vector |
| J | Current Density vector |
| $\rho$ | Charge density at any point. Also used as a general argument of a Bessel function |
| P | Electric polarization vector |
| M | Magnetic polarization vector |
| $\varepsilon_0$ | Electric Inductive capacity of free space defined by $D = \varepsilon_0 E$ |
| $\mu_0$ | Magnetic Inductive capacity of free space defined by $B = \mu_0 H$ |
| $\chi_m$ | Magnetic susceptibility $M = \chi_m H$ |
| $\chi_e$ | Electric susceptibility $P = \chi_e D$ |
| $\epsilon$ | Relative dielectric constant $= \frac{\varepsilon_1}{\varepsilon_0}$ |
| $K_m$ | Permeability $= \frac{\mu_1}{\mu_0}$ |
| A | Vector Potential of the Field |
| $\phi$ | Scalar Potential of the Field |
| $\Pi$ | Hertz vector, Electric Polarization Potential |
| $\Pi^*$ | Hertz vector, Magnetic Polarization Potential |
| $\sigma$ | Conductivity |

$w$ Surface density of charge, or charge per unit area

I Conduction current

i Square root of minus one

h Longitudinal propagation factor $= \frac{2\pi}{\lambda_1}$

t Time

e Base of natural logarithms

$J_n(\rho)$ Bessel Function of order n

$\rho$ An argument of a Bessel function

$Z_n(\rho)$ Circular cylinder function, or Bessel function, of order n

$N_n(\rho)$ Bessel function of the second kind

$H_n^{(1)}(\rho)$ Hankel function of the first kind

$K_n(\rho)$ Modified Bessel function

k Intrinsic phase constant $= \sqrt{\mu\varepsilon\omega^2 + i\mu\sigma\omega}$

$\omega$ Angular velocity = frequency/$2\pi$

$\chi_1$ A propagation constant for dielectric in the case of a circular cylinder in air $= \sqrt{k_1^2 - h^2}$

$\chi_2$ A propagation constant for air in the case of a circular cylinder in air $\sqrt{k_2^2 - h^2}$

p A propagation constant for dielectric $= \chi_1 a$

v A propagation constant for air in the case of a circular cylinder in air $= \chi_2 a$

a Radius of a circular cylinder of dielectric

q A propagation constant for air $= -iv = -i\chi_2 a = -ia\sqrt{k_2^2 - h^2}$

$n_a$ Apparent index of refraction for dielectric rod

$f$ Abbreviation for $\frac{J_n'(p)}{pJ_n(p)}$

$g$ Abbreviation for $\frac{K_n'(q)}{qK_n(q)}$

$\lambda_0$ Free space wavelength

$\lambda_1$ Wavelength of propagation in a dielectric antenna

$c$ Velocity of propagation in free space

$\ell_0$ Optimum length for dielectric to maximize on-axis radiation

# BIBLIOGRAPHY


1. Blanchard, Julian. "Hertz, the Discoverer of Electric Waves". Proc. I R E, May, 1938.

2. Linder, William J. "The Dielectric Rod Antenna". University of California Research Report, Navy Contract, NO bsr - 39401, Jan. 28, 1948.

3. Stratton J.A. "Electromagnetic Theory". McGraw-Hill Book Co., Inc., New York, 1941.

4. Schelkunoff, S.A. "Electromagnetic Waves." D. Van Nostrand Co., New York, 1943.

5. Silver, S. "Microwave Antenna Theory and Design". Vol. 12, M.I.T. Rad Lab Series.

6. Mallach, Peter. "Dielectric Directional Antennas for dm and cm Waves". Air Material Command Report F - TS - 2223 - RE, Feb., 1948. Translated by P.L. Harbury of Harvard University, Cambridge, Mass.

7. Southworth, G.C. "Some Fundamental Experiments with Waveguides". Proc. I R E., July, 1937.

8. Wilkes, Gilbert. "Wavelength Lenses". Bumblebee Series Report No. 59.

9. Elsasser, Walter M. "Attenuation in a Dielectric Circular Rod". J. App. Physics. Vol. 20, Dec., 1949.

10. Chandler, C.H. "An Investigation of Dielectric Rod as Wave Guide". J. App. Physics. Vol. 20, Dec., 1949.

11. Marston, A.E. "Radiation from Dielectric Rods of Uniform Circular Cross Section". Naval Research Lab Report 3757, Nov. 13, 1950.

12. McKinney, Chester M. "Dielectric Waveguides and Radiators". Bumblebee Series Report 138, Sept., 1950.

13. Wilkes, Gilbert. "Wave Length Lenses". Proc. I R E, Feb., 1948.

14. Horton C.W. "The Theory of the Radiation Patterns of Electromagnetic Horns". Bumblebee Series Report No. 86.

15. Spencer, R.C., and Austin, Pauline. "Tables and Methods of Calculation for Line Sources". M. I. T. Rad Lab Report, No. 762 - 2.

16. Horton, C.W. "On Dielectric Rod as an Antenna, Part II". University of Texas, Defense Research Lab Report No. 91, C T 481, Nov. 8, 1946.

17. Wilkes, Gilbert. "Lentilles Ayant Une Dimension De L'Ordre D' Une Longeur D'Orde". Extrait des Comptes rendus des seances de l'Academie des Scienses, seance du decembre, 1946. French.

18. Schelkunoff, S.A. "Some Equivalence Theorems of Electromagnetics". B.S.T.J. Vol. 15. Jan., 1936.

19. Phillips, H.B. "Vector Analysis". John Wiley and Sons, New York.

20. Cutler, King and Kock. "Microwave Antenna Measurements". IRE Proceedings, Dec., 1947.

21. Zinke et Mallach. "Les Antennes Dielectriques". L'Onde Electrique, Octobre, 1946. French.

22. Slater, J.C. "Microwave Transmission". McGraw-Hill Book Co., New York.

23. Jordan, Edward C. "Electromagnetic Waves and Radiating Systems". Prentice-Hall, Inc., New York.

24. Wilkes, Gilbert. "An Experimental Investigation of the Interaction of Radiant Energy". Johns Hopkins University, Applied Physics Lab. Report under preparation.

25. Second Quarterly Progress Report. "Millimeter Wavelength Antenna Studies". by Stanford Research Institute for U.S. Army Signal Corps, 30 Sept., 1951.

26. Mandelker, Jakob. "A New Theory of Gravitation". Philosophical Library, New York, 1951.

27. de Broglie, Louis. "Méchanique Ondulatoire du Photon et Théorie Quantique des Champs". Paris, 1948.

# VITA

Robert Bruce Johnston was born in Asheville, N.C., November 17, 1912; graduated from the Georgia School of Technology in 1934, with the degree of Bachelor of Science in General Science; and was employed after graduation at the American Enka Corporation, Enka, N.C. until the outbreak of World War II. In February, 1942, he was commissioned Ensign in the U.S. Naval Reserve and was assigned to Harvard University for a brief course in Radio Engineering, followed by three month's instruction in Radar at the Massachusetts Institute of Technology. For the next three years he served in the Navy Bureau of Ordnance in Administration of Fire Control Radar Maintenance, after which he went aboard the U.S.S. Lexington (CV16) for duties as electronics maintenance officer. In September, 1946, Lieutenant Commander Johnston transferred to the regular Navy and was assigned to the Navy Bureau of Ships, Electronics Division, Design Branch, as head of the Fire Control Radar design section. Following this he was again assigned to the Bureau of Ordnance for duty as procurement officer for Guided Missiles, where he served until entering the U.S. Naval Postgraduate School in 1949. At the Postgraduate School in Annapolis he studied Ordnance Engineering, specializing in Guided Missile Control, and in June, 1951, was awarded the degree of Bachelor of Science in Electrical Engineering. During the three months preceding his entrance to the Johns Hopkins University, he was assigned to the Johns Hopkins Applied Physics Laboratory in Silver Spring, Maryland. It was during this summer visit to the laboratory that problems connected with dielectric antennas were brought to his attention, which led to the experiments outlined in this paper.

18040

Thesis J67

Johnston

An experimental investigation of the gains of dielectric antennas.